



Contents lists available at ScienceDirect

Arabian Journal of Chemistry

journal homepage: www.ksu.edu.sa

Advances in synthesis of the graphene quantum dots from varied raw materials

Yong Huang^{a,b,*}, Danping Wang^{a,b}, Yali Wei^{a,b}, Xin Dong^{a,c}, Rong Yang^{a,c,*}, Haoyun Li^d, Minqi Wei^{a,c}, Jie Yu^{a,c}, Lisheng Zhong^{a,c}, Yunhua Xu^{a,c,e}

^a International Research Center for Composite and Intelligent Manufacturing Technology, Institute of Chemical Power Sources, Xi'an University of Technology, Xi'an 710048, China

^b Faculty of Humanities and Foreign Languages, Xi'an University of Technology, Xi'an 710048, China

^c College of Materials Science and Engineering, Xi'an University of Technology, Xi'an 710048, China

^d Shaanxi Hongma Science and Technology Co., Ltd, China

^e Yulin University, Yulin 719000, China

ARTICLE INFO

Keywords:

Graphene quantum dots
Raw material
Graphite
Coal
Organic small molecules

ABSTRACT

As a new type of carbon material, graphene quantum dots (GQDs) show potential application value in chemical catalysis, biomedicine, optoelectronics, energy and other related fields because of its stronger quantum confinement effect and edge effect. Therefore, the preparation and application of GQDs have become one of the hotspots in the research of graphene-based materials. From the published references on the synthesis and applications of GQDs, it can be seen that the difference of raw materials is still one of the important factors which affects the size, functional groups, fluorescence properties, and yields of GQDs, in addition the methods. In order to reduce the preparation cost and develop efficient and green methods to obtain GQDs, this review emphasized the differences in size and fluorescence properties of GQDs prepared by different raw materials such as graphite, coal, coke, as well as organic small molecules and biomass, and the reasons for the differences. Specifically, the advantages and disadvantages of different raw materials related preparation methods of GQDs are compared. Finally, an outlook on the possible solutions to the existing problems and the future research directions on preparation methods of GQDs with high yield and quality is proposed.

1. Introduction

Graphene quantum dots (GQDs) are a new type of zero-dimensional carbon material consisting of graphene sheets with lateral dimensions less than 100 nm (Li et al., 2015; Shi et al., 2023; Ham et al., 2023; Zhu et al., 2022). Compared with graphene, GQDs exhibit strong quantum-limited and edge effects (Ritter and Lyding, 2009; Fan et al., 2023; Fan et al., 2023) that give them many advantages, such as stable fluorescence properties (Carrasco et al., 2016; Vázquez-Nakagawa et al., 2022; Kharangarh et al., 2023; Qin et al., 2023), low cellular toxicity (Zhang et al., 2022; Reghunath et al., 2023), and good water solubility (Hsieh et al., 2023; Zeng et al., 2022). Therefore, GQDs have comprehensive applications in many fields such as optoelectronic devices (Mahalingam et al., 2023), sensors (Kolhe et al., 2023; Chang et al., 2023); bioimaging (Yan et al., 2023; Chung et al., 2021), drug transport (Kurniawan et al., 2023), energy (Kharangarh et al., 2022; Kharangarh et al., 2020) and

environmental detection (Kurniawan et al., 2022), etc. In addition, GQDs can be modified by heteroatom doping (Kurniawan et al., 2023; Martins et al., 2023), surface functionalization (Kurniawan et al., 2022; Martins et al., 2023; Tetsuka et al., 2012), and decorated/composited to obtain nanocomposites (Kharangarh et al., 2021; Kharangarh and Singh, 2023) and tune the material properties, (e.g., electrocatalytic activity (Tetsuka et al., 2012; Han et al., 2023), optical properties (Liu et al., 2017; Kharangarh et al., 2018; Papari et al., 2017), water solubility (Yan et al., 2010), etc.) which makes them more widely applicable.

There are various methods for the synthesis of GQDs, which are mainly divided into two categories: top-down technique and bottom-up method. Top-down method to prepare GQDs generally use graphite, carbon nanofiber, graphite oxide, coal, etc. as raw materials by oxidation, shearing or exfoliation (Kharangarh et al., 2021; Kharangarh and Singh, 2023; Han et al., 2023). The above raw materials are carbon materials with large sp^2 carbon domains and are abundant in sources

* Corresponding authors.

E-mail addresses: huangy01@xaut.edu.cn (Y. Huang), yangrong@xaut.edu.cn (R. Yang).

<https://doi.org/10.1016/j.arabjc.2023.105533>

Received 5 August 2023; Accepted 4 December 2023

Available online 7 December 2023

1878-5352/© 2023 The Authors. Published by Elsevier B.V. on behalf of King Saud University. This is an open access article under the CC BY-NC-ND license (<http://creativecommons.org/licenses/by-nc-nd/4.0/>).

and easy to prepare. Due to sufficient raw materials and easy to operate, researchers are trying to develop top-down methods for large-scale production of GQDs. Meanwhile, the edges of this route for synthesizing GQDs contain a large number of oxygen-containing functional groups, which not only promotes the solubility of GQDs, but also creates conditions for functionalization and passivation. However, this method also has some shortcomings, such as special requirements for instruments and equipment, low production, damage to the benzene ring structure, and the lack of selectivity in obtaining GQDs from top to bottom. Therefore, precise control of its morphology and particle size distribution cannot be achieved. Bottom-up method, on the other hand, employs organic small molecules such as citric acid or aromatic molecules as raw materials to prepare GQDs by controlled synthesis methods such as hydrothermal/solvent thermal environments or carbonization methods (Yan et al., 2010; Yan et al., 2018; Bayat and Saievar-Iranizad, 2017). Such methods facilitate effective size control of GQDs, but often require the selection of specific organic materials as raw materials and undergo complex reaction steps. There are also some examples of GQDs prepared by special methods or raw materials, such as Lu et al. (Lu et al., 2011) who used ruthenium as a catalyst to catalyze the opening cage of fullerenes to obtain a small amount of GQDs, and Wang et al. (Wang et al., 2011) who separated GQDs from GO by selective precipitation. The specific methods for preparing GQDs vary with the structure of different raw materials, thus the size, fluorescence properties, and yields of the resulting GQDs are also different.

The currently obtained GQDs is usually hydrophilic. Actually, in the field of optoelectronics, conventional manufacturing processes tend to make materials more soluble in organic media. A new method for

preparing hydrophobic GQDs is needed. On the other hand, for the sensing and Biomarker application of GQDs, specific surface functionalization is usually inevitable. In order to reduce the preparation cost and develop efficient and green methods of GQDs, this review emphasized the differences in size and fluorescence properties of GQDs prepared by different raw materials such as graphite, coal, coke, as well as organic small molecules and biomass in Fig. 1, and the reasons for the differences, compares the advantages and disadvantages of different raw materials related preparation methods of GQDs, proposes possible solutions to the existing problems, and gives an outlook on the future research directions to meet the need of developing new ways to efficiently and conveniently prepare GQDs with high yield, high quality, specific properties and functions to promote their practical applications in the future.

2. Graphite

Graphite is one of the isomers of carbon, which has a regular layer structure and good electrical and mechanical properties. Due to the large spacing of graphite layers and the weak interlayer forces, it is easy to be peeled into thinner graphite flakes. Graphene is a sheet of graphite that is only one carbon atom thick. GQDs are obtained by “cutting” graphene to a size of about 10 nm.

2.1. Graphite and graphene as raw materials

Based on the good electrical conductivity of graphite, Zhang et al. (Zhang et al., 2012) obtained GQDs with a large number of hydrazide

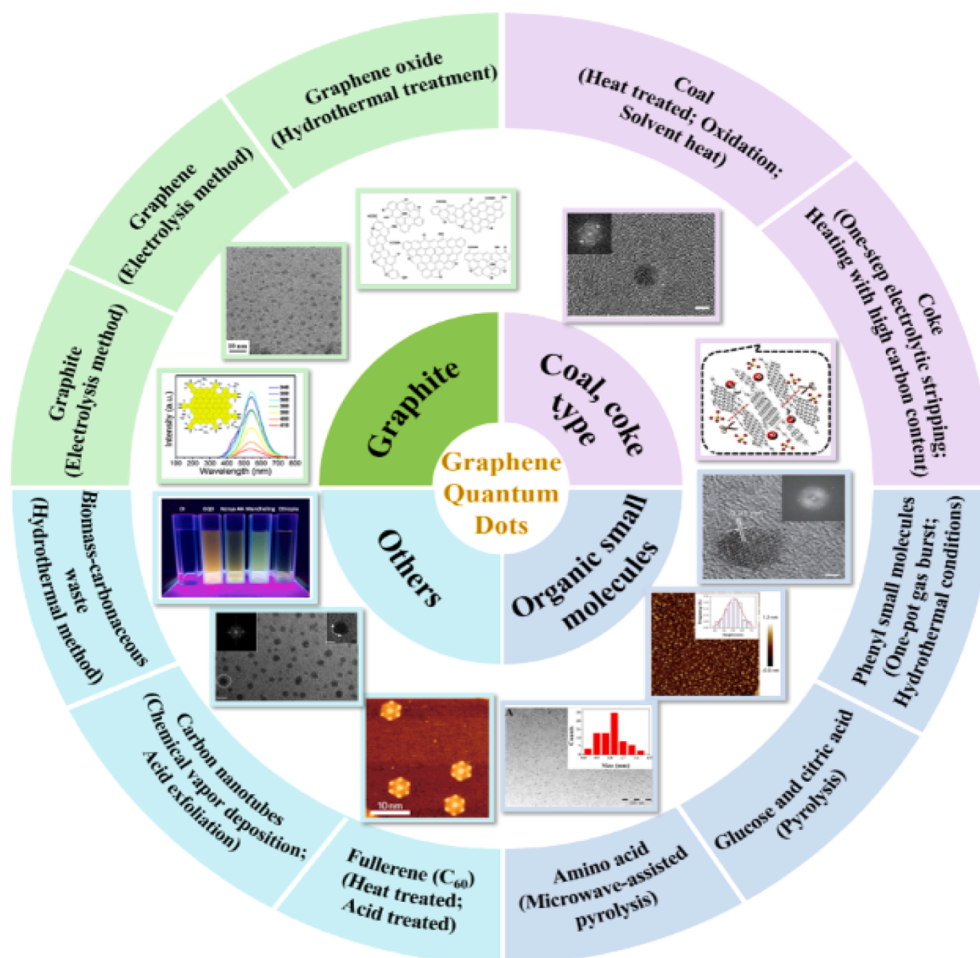


Fig. 1. Schematic illustration of raw materials and methods for preparing graphene quantum dots.

groups at the edges by electrolytic exfoliation of graphite rods as an anode in aqueous NaOH solution, followed by reduction with hydrazine hydrate at room temperature (Fig. 2a). TEM (Transmission Electron Microscope) result shows GQDs thickness <0.5 nm with average size of 5–10 nm is consistent with monolayer graphene's. The GQDs can excite bright yellow fluorescence in aqueous solution at pH = 7 with a quantum yield of 14 %.

Ahirwar et al. (Ahirwar et al., 2017) also used graphite rods as electrodes, with the difference that the electrolyte solution was electrolyzed with citric acid and NaOH. GQDs with an average size of 2.2–3.0 nm and emitting blue-green fluorescence under 365 nm UV light were obtained by varying the amount of electrolyte NaOH. The authors obtained the mechanism of preparing GQDs by electrochemical exfoliation by heating the pristine graphite rods at 1050 °C for 5 min to obtain defect-induced graphite rods as electrodes (as shown in Fig. 2b). During electrochemical exfoliation, cutting and oxidation occur at the defect sites, and the more defects, the more cutting and oxidation sites; When the electric potential is applied, the OH^- ions of water dissociation are embedded between the graphite layers, which are oxidized to oxygen at the defect sites. OH^- ions and oxygen occupy the van der Waals gap, leading to the flaking of defective graphite rods (anodes) as GQDs.

Compared to graphite, graphene has fewer carbon layers and therefore is easier to peel and cut. Li et al. (Li et al., 2011) used graphene films as working electrodes and electrolyzed a homogeneous solution of GQDs in 0.1 mol/L phosphate solution, which showed good stability without agglomeration or color change for 3 months at room temperature. This GQDs were examined by TEM and AFM (Atomic Force Microscope), and the results showed that the average size of the GQDs was 3–5 nm, and the morphological height was between 1 and 2 nm, with about 1–3 graphene single atomic layers. The fluorescence detection results showed that the GQDs can excite green fluorescence at 365 nm, and their use in photovoltaic conversion devices can improve the conversion efficiency. Ananthanarayanan et al. (Ananthanarayanan et al., 2014) used acetonitrile solution of 1-butyl-3-methylimidazolium hexafluorophosphate (BMIMPF₆) as the electrolyte solution to electrolyze self-supported foam-like 3D graphene assembled based on chemical vapor deposition in Fig. 2c. The average size of the prepared GQDs is

around 3 nm, which is mainly the thickness of monolayer graphene, and the GQDs can be excited with blue fluorescence under UV light at 365 nm with a quantum yield of about 10 % when quinine sulfate is used as the standard reference.

It can be seen that based on the excellent electrical conductivity of graphite and graphene and using them as raw materials, the GQDs obtained by a simple, reliable and reproducible electrolytic method are generally smaller than 5 nm with uniform size and stable performance; the surface of GQDs is rich in hydroxyl and carboxyl functional groups, which makes them soluble in aqueous media and also helps to further functionalize and develop various applications. Meanwhile, the exfoliation and cutting of GQDs from graphite as the starting material also has the advantage of high reaction yields (>70 wt%). It is generally believed that graphene-based GQDs perform better than graphite-based GQDs. the reason is that graphene has fewer layers compared to graphite, and it is easier to exfoliate and break to obtain GQDs with smaller size and thickness during electrolysis, but the good performance of graphene itself is currently facing the status of expensive preparation equipment or complicated process, which in turn increases the cost of preparing GQDs.

2.2. Graphene oxide as a starting material

Graphene oxide (GO) is an oxide of graphene with oxygen-containing functional groups such as hydroxyl and carboxyl groups on its surface, which can provide active sites for chemical reactions. Therefore, GO is easier to “cut” to obtain GQDs than graphite and graphene, and it is also easy to complete the modulation and modification of GQDs functional groups at the same time.

Wu et al. (Wu et al., 2016) synthesized nanoscale GO by a modified Hummers method (Chen et al., 2013), and then performed hydrothermal treatment at different temperatures with different concentrations of ammonia to obtain high-quality GQDs with tunable fluorescence properties from hydrophilic to hydrophobic and from blue to yellow, while achieving high yields of 60 wt% and 18.2 % fluorescence quantum yields (Fig. 3a). Pan et al. (Pan et al., 2012) “cut” monolayers of GO into fluorescent GQDs in three steps: First the monolayer GO was converted into chemically derived graphene flakes by thermal reduction; then the

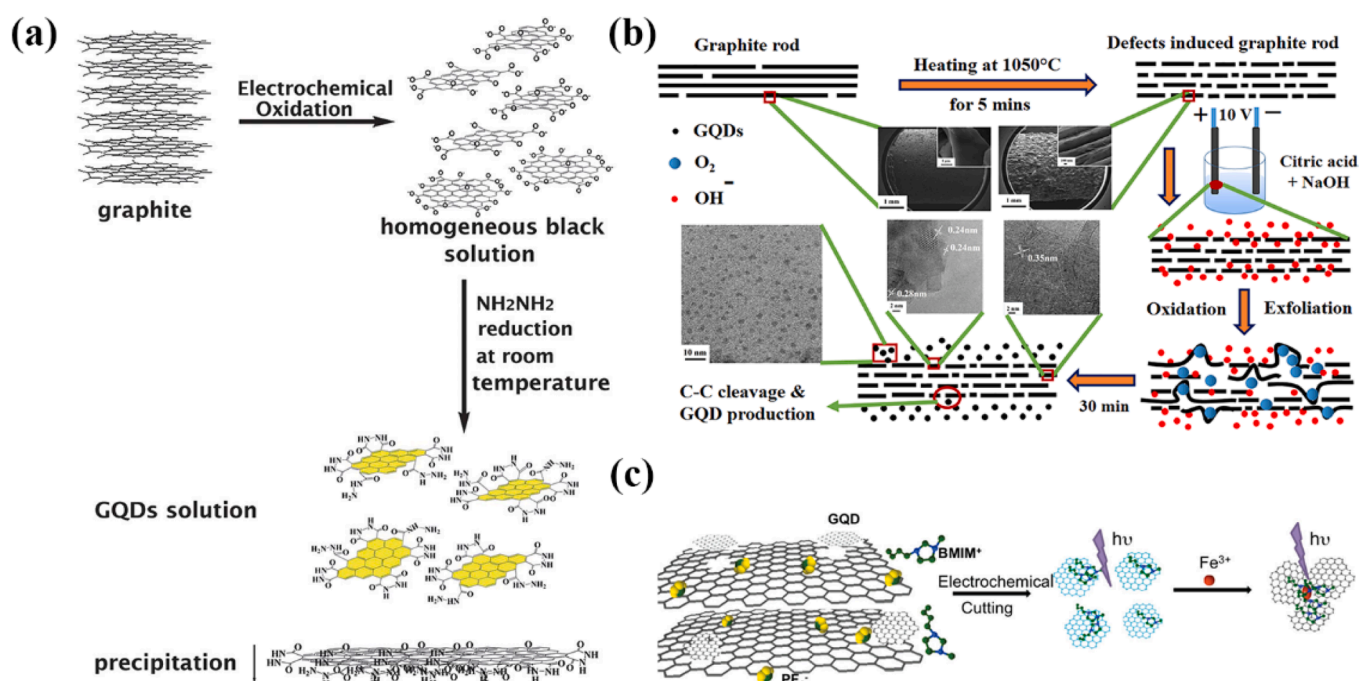


Fig. 2. (a) Schematic illustration of the generation process of GQDs solution. Reproduced with permission (Zhang et al., 2012). (b) Schematic illustration of electrochemical exfoliation of defect-induced graphite rod. Reproduced with permission (Ahirwar et al., 2017). (c) Schematic illustration of GQD synthesis from 3D graphene and mechanism of Fe^{3+} detection. Reproduced with permission (Ananthanarayanan et al., 2014).

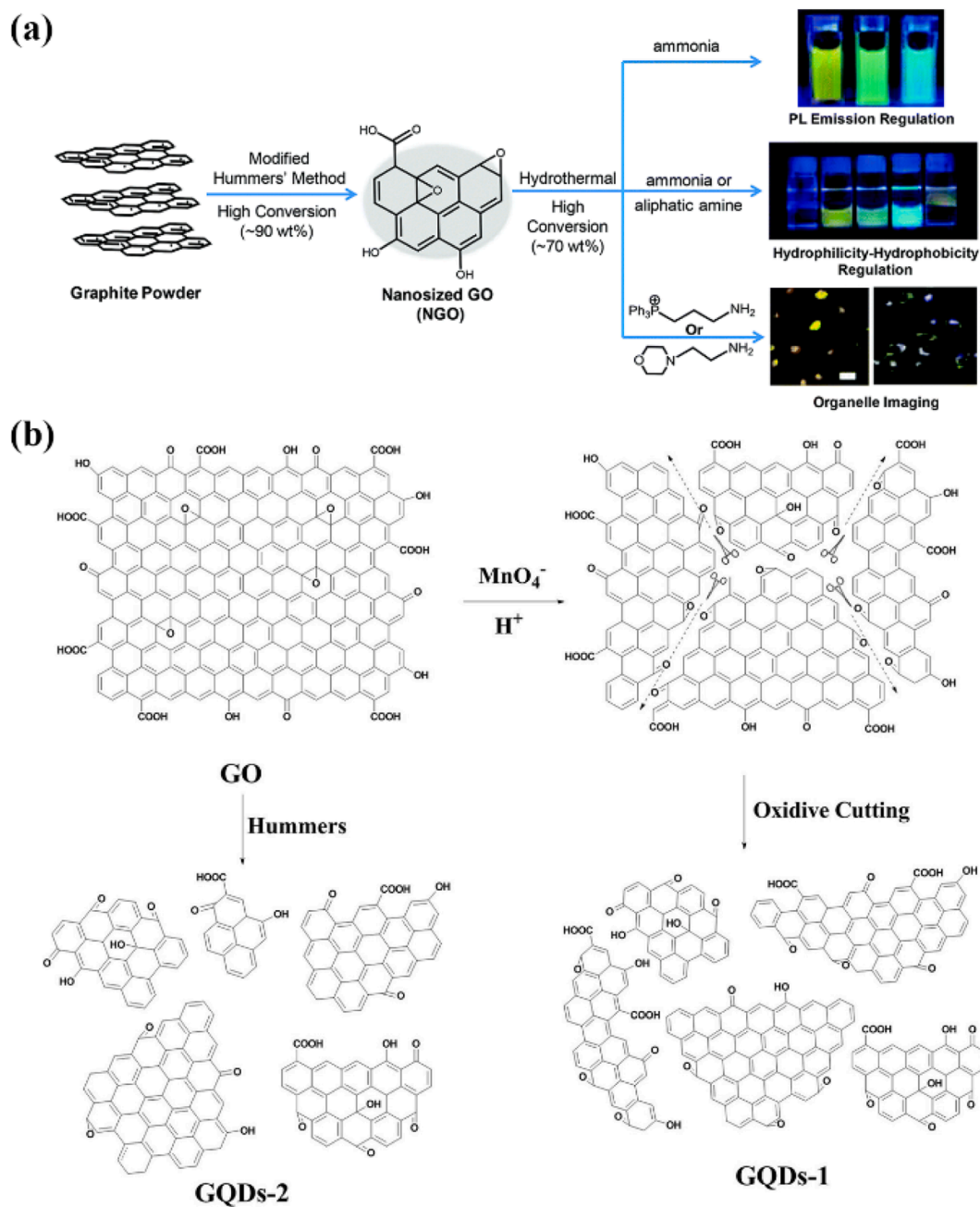


Fig. 3. (a) Schematic illustration of the high-efficient preparation processes for GQDs with diverse properties. Reproduced with permission (Wu et al., 2016). (b) Mechanism of fabricated GQDs-1 and GQDs-2 for cutting GO by modified Hummer's method. Reproduced with permission (Fan et al., 2015).

graphene flakes were oxidized in a mixture solution of concentrated sulfuric acid and nitric acid; finally, the oxidized graphene flakes were subjected to a strong alkaline hydrothermal reaction at pH > 12 for 10–12 h to produce GQDs with intense green light. The authors suggest that the oxidation step can induce the production of carboxyl groups (—COOH) at the edge or cavity positions and carbonyl groups (C=O) and epoxy groups (C—O—C) at the basal positions. Epoxy groups and carbonyl groups tend to form linear chains and enclose a few nanometers sp^2 clusters with lateral dimensions. The linear chains are opened and removed in the subsequent alkaline hydrothermal reaction, while the relatively stable carboxyl groups are retained, resulting in water-soluble GQDs with carboxyl functionalization. The above-mentioned “fine chemical cutting” route using high-temperature thermally reduced GO sheets as precursors resulted in the preparation of ultra-small GQDs with high crystallinity of 1.5–5 nm transverse dimension

and 2–3 single atomic layers longitudinally, making them potentially useful in the electronic and optoelectronic fields.

Fan et al. (Fan et al., 2015) fabricated GO powder with a diameter of about 10 nm by a modified Hummers method, then suspended it in concentrated sulfuric acid and obtained two different sizes of GQDs-1 and GQDs-2 in one step by varying the addition of $KMnO_4$ (as shown in Fig. 3b). This method can regulate the size of GQDs in the range of 2–4 and 3–5 nm and simultaneously adjust their edge structures by oxidative cutting. The obtained GQDs all have size-dependent fluorescence properties with quantum yields as high as 34.8%. Zhao et al. (Zhao, 2018) used a three-step hydrothermal etching to GO precursors and obtained two GQDs with average diameters of 3.38 nm and 2.03 nm after treatment with different concentrations of nitric acid. Under 365 nm UV excitation, the two GQDs exhibited green and yellow luminescence; The HNO_3 oxidation led to the introduction of N atoms and

oxygen-containing groups, and N atoms were doped in GQDs in the form of C–N–C and N–(C)₃ and –NO₂. The GQDs exhibited different optical properties, which were attributed to the differences in the degree of oxidation and nitrogen doping.

The epoxy functional group in GO is often found on the C–C bond, which is very active and can easily undergo ring-opening reactions, resulting in the easy cutting of GO and the formation of small-sized GQDs. Therefore, by using GO as the raw material, the size, oxidation degree of quantum dots and the functional groups can be adjusted by changing the amount of oxidant added or the acidity or alkalinity of the reaction and the time, thus adjusting the fluorescence properties of quantum dots or changing the hydrophilic and hydrophobic properties. Compared with graphite, GO can be used as raw material to obtain high quality GQDs with smaller size and higher quantum yield. However, the preparation process requires strong acid and strong oxidizing agent, which needs to be neutralized in the post-treatment. At the same time, the GQDs also retain or remain part of the oxygen-containing groups of GO, which may require subsequent reduction steps. The whole preparation process takes a long time to separate and purify that affects the preparation efficiency.

3. Coal, coke type

Coal is the most abundant natural resource, mainly composed of carbon, hydrogen, oxygen, nitrogen and sulfur, among which carbon, hydrogen and oxygen account for about 95 % or more, and has graphite-like cluster structure. Coal is generally divided into three categories: lignite, bituminous coal and anthracite, and the graphitization degree of different types of coal varies. Compared with graphite, coal has an inherent disordered structure, so it is easy to exfoliate, and then through simple chemical treatment to achieve oxidative cleavage, graphite structure can be extracted from coal to produce carbon nanomaterials.

3.1. Coal as raw materials

Structurally, lignite is mainly a single or double thick ring aromatic,

while anthracite usually has more than ten thick rings. Xu et al. (Xu et al., 2018) prepared GQDs from several raw coals with low to high graphitization, such as lignite, coking coal (a type of bituminous coal), and anthracite, using one-pot hydrothermal and dialysis, and doping with N, P, and S atoms at the edges of the structure (Fig. 4a). The experimental results showed that the diameter distribution of GQDs obtained from the anthracite coals with high graphitization degree was 1–7 nm, and the diameter of GQDs from coking coal was 1–3 nm, while only broken carbon flakes instead of GQDs could be obtained from lignite due to low graphitization degree during the oxidation cutting process. The Raman spectroscopy results showed that the defects and disorder of the obtained GQDs increased gradually during the conversion of the coals into nano-GQDs. The raw coal with too high or too low graphitization is not the best raw material for generating high-quality GQDs. It was also reported in the literature that Ye et al. (Ye et al., 2013) obtained GQDs from anthracite, bituminous coal, and coke by sonication with mixed acids (concentrated sulfuric acid and concentrated nitric acid) and heating, respectively. It was found that it was relatively easy to synthesize GQDs from bituminous coal because the connection between the nano-graphitized carbon domains and amorphous carbon in bituminous coal was weak and easily cleaved during the oxidation process (e.g., Fig. 4b–g). That is, the crystalline carbon in the coal structure was more easily replaced by oxidation than the carbon of the pure sp² structure, resulting in GQDs with nano-sized, amorphous carbon edges. This reported the yield of GQDs isolated from coal was 20 %.

Ghorai et al. (Ghorai et al., 2018) developed a cost-effective oxidation method for the preparation of GQDs from bituminous coal, no strong acid was used in the solvent heat process, the purification process was salt-free, and the yield was up to about 45 % (Fig. 4h). The coal was first heat treated with concentrated hydrochloric acid for 2 h and then cooled to room temperature, filtered and washed several times (to remove the free acid), and then oxidized with concentrated nitric acid at 90 °C for 6 h. After removing the excess acid by vacuum distillation, the coal was then treated by solvent heat with N, N-dimethylformamide (DMF) as the solvent and monopersulfate of potassium as a neutral oxidant at 220 °C for 8 h. Based on the combined effect of heating

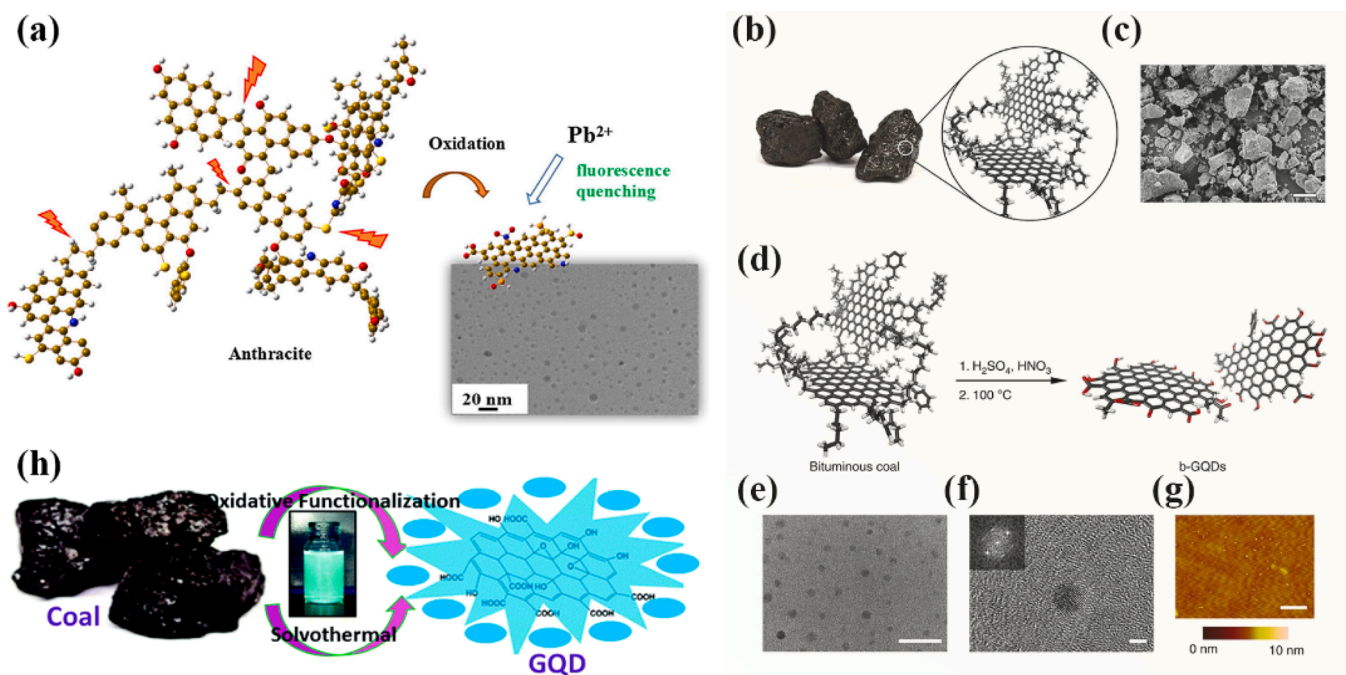


Fig. 4. (a) An illustration of the formation process of the NPS-GQDs. Reproduced with permission (Xu et al., 2018). (b) Macroscale image and simplified illustrative nanostructure of coal. (c) SEM image of ground bituminous coal with sizes ranging from 1 to hundreds of microns in diameter. Scale bar, 50 mm. (d–g) Schematic illustration of the synthesis of b-GQDs and its micro-morphology characterization. Reproduced with permission (Ye et al., 2013). (h) Schematic representation of the synthesis of GQDs from coal. Reproduced with permission (Ghorai et al., 2018).

oxidation cutting and the raw coal edge defects, GQDs with high crystallinity, narrow size distribution (2.5–5 nm) and high-intensity blue fluorescence were obtained with a quantum yield of 14.42 %.

In addition, since the cavitation effect of ultrasonic waves in liquids can lead to high local temperatures, this high-energy environment can trigger thermal decomposition. Zhang et al. (Zhang et al., 2019) used an ultrasonic cell crusher to disperse unacid-treated anthracite powder with a high degree of kerogenization into DMF, and hydrogen bonds were rapidly formed between oxygen-containing groups (e.g., hydroxyl and carboxyl groups) of DMF molecules and coal molecules. Subsequently, the suspension was subjected to ultrasonic treatment in an ultrasonic cell crusher. This high-energy environment triggered a series of chemical reactions (e.g., thermal decomposition and dissociation) to break the bridge bonds and create new oxygen-containing groups at the edges of the coal molecules. They could quickly combine with DMF molecules and form hydrogen bonds to avoid the restoration of bridge bonds (e.g., Fig. 5). The final micron-sized coal powder was broken into nano-GQDs with blue fluorescence. Separation dialysis yielded GQDs with an average diameter of 3.2 ± 1.0 nm and a quantum yield of 5.98 %. The obtained GQDs were reduced with NaBH_4 to prepare fluorescent probes that can be quenched by Cu^{2+} , which can be used for Cu^{2+} detection in water.

As seen above, it is feasible and effective to prepare GQDs from coal, which is rich in natural resources and cheap and economical. Since the degree of graphitization varies among different types of coal, bituminous coal with weak connection between the nano-graphitized carbon domains and amorphous carbon or anthracite coal with relatively high graphitization can be generally used, and the common method is chemical oxidative etching. However, the reaction conditions are more restrictive, such as the need to react in concentrated sulfuric and nitric acids, as well as higher temperatures and longer reaction times. In addition, acid oxidation induces a large number of oxygen-containing groups, which drastically reduces the size of the sp^2 conjugated carbon in the coal matrix, leading to a weakening of the fluorescence intensity

of GQDs. If the quantum yield requirement is not high, the graphitized anthracite coal can be used as raw material and ultrasonicated after organic solvent DMF dispersion, which avoids the use of strong oxidant and the subsequent neutralization step, and the method is greener and environmentally friendly. It is conducive to the value-added utilization of coal resources.

3.2. Coke as raw material

Coke is produced by high-temperature coking of anthracite coal, and a certain amount of coal tar is also obtained during the coking process. Coke has a higher degree of graphitization compared to coal.

Yew et al. (Yew et al., 2017) reported coke-derived GQDs, which were obtained from calcined petroleum coke by ultrasonication for 2 h and then dispersed in a mixture of concentrated sulfuric acid and concentrated nitric acid at 100 °C for 24 h. In-depth studies, they revealed that fluorescence quenching occurred when DNA accumulated on the surface of GQDs through hydrophobic interactions, and thus coke-derived GQDs could be used as DNA detectors. He et al. (He et al., 2018) assembled a variety of GQDs with tunable fluorescence properties using a one-step electrolytic stripping of coke. Platinum electrode was used as the counter electrode and coke as the working electrode at pH = 7.0 with a current density range of 80 $\text{mA}/\text{cm}^2 \sim 400 \text{ mA}/\text{cm}^2$, a mixture of methanol and deionized water as the solvent, and ammonium persulfate ($(\text{NH}_4)_2\text{S}_2\text{O}_8$) as the electrolyte. By varying the ratio of methanol to water and the current density applied to the coke, O-GQDs emitting orange fluorescence, green G-GQDs and yellow Y-GQDs were obtained, followed by the reduction of G-GQDs with NaBH_4 as the reducing agent to obtain blue fluorescence B-GQDs (Fig. 6a). During the electrochemical stripping of coke, for example, the electrolyte gradually changed from colorless to light yellow during the initial stripping stage of Y-GQDs, and then the coke anode swelled slightly and made the electrolyte darker. Finally, swellable flakes and particles fall from the coke anode and form a dark yellow slurry. These three distinct

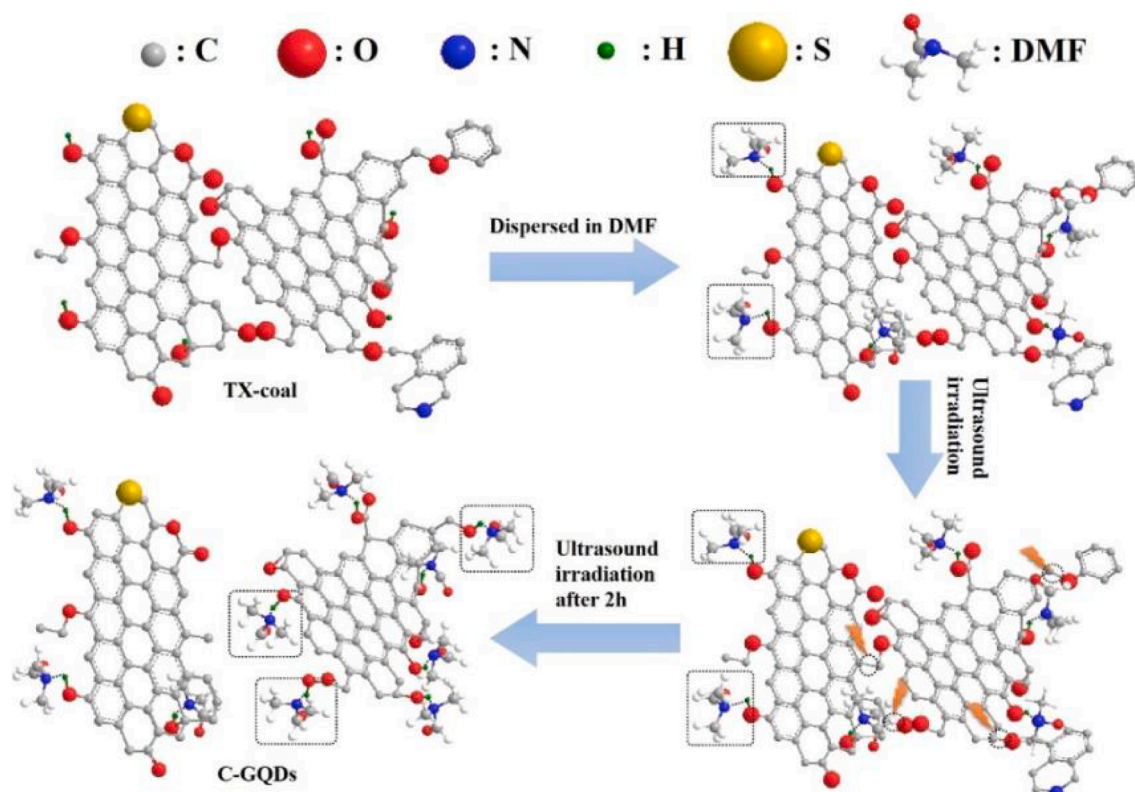


Fig. 5. Schematic illustration of C-GQDs synthesis. Reproduced with permission (Zhang et al., 2019).

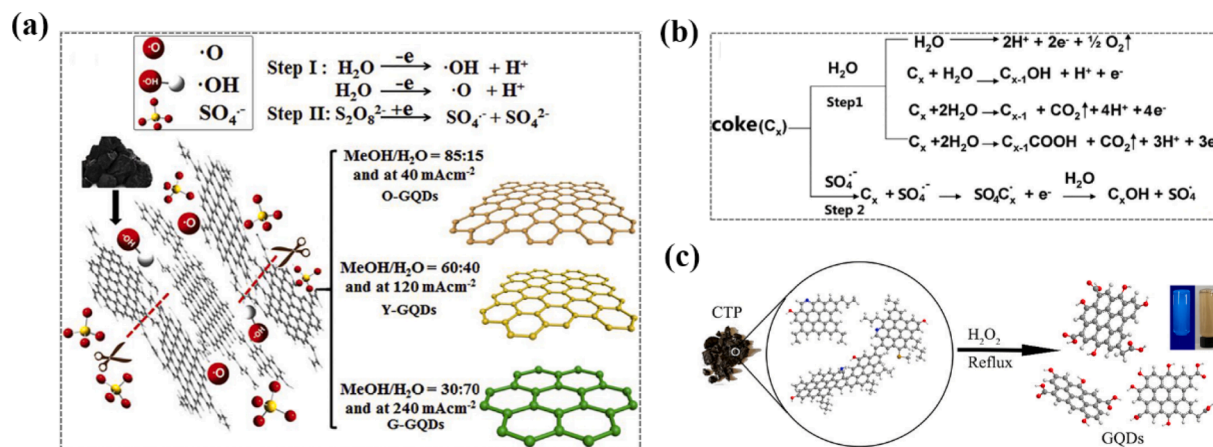


Fig. 6. (a) Photo of the exfoliated process showing the attack of the coke edge planes by $\cdot\text{OH}$ and $\cdot\text{O}$ radicals, which benefits the insertion of SO_4^{2-} . (b) The anodic oxidation of H_2O (step 1) and intercalation of SO_4^{2-} (step 2) cause together the formation of the stripped products. Reproduced with permission (He et al., 2018). (c) Schematic illustration of the fabrication of GQDs. Reproduced with permission (Liu et al., 2018).

phenomena correspond to the different dynamic electrolytic processes of electrochemical oxidation, embedding and swelling, respectively. During the decomposition process, a large number of O_2 bubbles generated by water decomposition were observed at the anode. O-, Y-, G- and B-GQDs with yields up to 31.13 wt%, 42.86 wt%, 17.88 wt% and 13.04 wt % were finally obtained with relative quantum yields of 9.24 %, 7.90 %, 8.47 % and 19.27 %, respectively.

The authors confirmed that the electrochemical exfoliation of coke consists of two key steps. As shown in Fig. 6b, step I can be designated as the conventional electrochemical “shearing” stage, where the $\cdot\text{OH}$ and $\cdot\text{O}$ radicals generated from water decomposition act as electrochemical “scissors” to exfoliate the coke into multilayer graphene flakes by efficient electrochemical oxidative cleavage. During electrolysis, the reactive $\cdot\text{OH}$ and $\cdot\text{O}$ radicals violently impinge on the coke edge planes and greatly accelerate the edge hydroxylation or oxidation process, which significantly promotes the edge planes to unfold more edge flake layers. The open edge lamellae make it easier for the SO_4 radicals to insert into the lamellae. By making the lamellae be separated, the resulting products swell along the stacking direction, favorably breaking the weaker aliphatic C—C bonds. However, the stronger aromatic C—C bonds remain intact in most cases, agglomerating to form nano-GQDs. Thus, other things being equal, the increased H_2O will be electrolyzed and produce higher concentrations of $\cdot\text{OH}$ and $\cdot\text{O}$ radicals. The large number of radicals strongly shear the coke into smaller graphene sheets, which are then further stripped by SO_4 radicals into more nano-GQDs with blue fluorescence.

Coal Tar Pitch (CTP) is a by-product of the coking industry with a unique structure consisting of an aromatic nucleus linked to several short-chain hydrocarbon groups, which is very similar to the structure of GQDs. Based on this, Liu et al. (Liu et al., 2018) used a simple and mild method to produce GQDs with an average size of 1.7 ± 0.4 nm and blue fluorescence at 328 nm by heating CTP with high carbon content (93.54 %) and H_2O_2 as the oxidant for 2 h and the yield of GQDs was more than 80 % (Fig. 6c). This simple preparation method with inexpensive raw materials, green reagents, mild reaction conditions and high yields provides a feasible way for the commercial synthesis of GQDs.

When coke is used as the raw material for the preparation of GQDs, the electrolysis method has the significant advantages of mild and easy controlling reaction conditions, faster preparation speed and higher preparation yield compared with the strong acid oxidation method. When CTP is used as the raw material, GQDs can be produced by reacting with H_2O_2 oxidant under mild conditions without complicated instrumentation because of its rich branched chains and the inherent structural advantage of amorphous carbon at the edge of the molecule. Since coke and its refining by-products are widely available,

economically priced, fast and convenient in the preparation of GQDs, they have some potential applications in the large-scale preparation of coke-based GQDs. The above GQDs prepared by either electrochemical electrolysis or H_2O_2 oxidant method have common features: The edges are rich in oxygen-containing functional groups, which are highly soluble in aqueous solution.

4. Organic small molecules

GQDs can be fabricated by top-down crushing and cutting from graphite and coke as raw materials, in addition to bottom-up splicing from organic small molecules. Various phenyl molecules, glucose, citric acid and amino acids are commonly used as raw materials for the preparation of GQDs. For example, GQDs with high quantum efficiency (QY) can be synthesized by hydrothermal methods such as using citric acid and binary or ternary amines. Organic small molecules are widely available, easy to design structures and simple synthesis processes. They are suitable for controlling the size of GQDs but requires multi-step organic reactions and purification at each step.

4.1. Phenyl molecules as starting materials

Phenyl molecules can be used as raw materials for the synthesis of GQDs due to their high carbon content and six-membered ring structure. Toluene and hexabromobenzene were published to fuse under sodium catalysis to produce GQDs without chemical groups (Yan et al., 2018). However, because of the activity of sodium and the carcinogenicity of toluene, the synthesis needs to be very careful and there is by-product generation of graphene nanoribbons. Li et al. (Yan et al., 2010) made GQDs containing 168, 132 and 170 conjugated carbon atoms by solution chemistry based on oxidative condensation reaction using 3-iodo-4-bromoaniline as precursor (Fig. 7a). The authors attached multiple 2',4',6'-trialkyl substituting benzene rings to the edges of GQDs, and the crowding of the graphene core edges distorted the substituted phenyl groups from the plane of the core, resulting in the closure of the latter in all three dimensions by the alkyl chains. It prevents product aggregation and reduces face-to-face interactions between graphene, thus effectively increases their solubility and also obtains GQDs with uniform, adjustable size and stability.

The gram-scale synthesis of single-crystal GQDs can be performed by a simple molecular fusion route under mild and green hydrothermal conditions in Fig. 7b (Wang et al., 2014). The synthesis process includes nitration of pyrene followed by hydrothermal treatment in alkaline aqueous solutions where the alkaline material plays a key role in regulating their size, functionalization and optical properties. Single-crystal

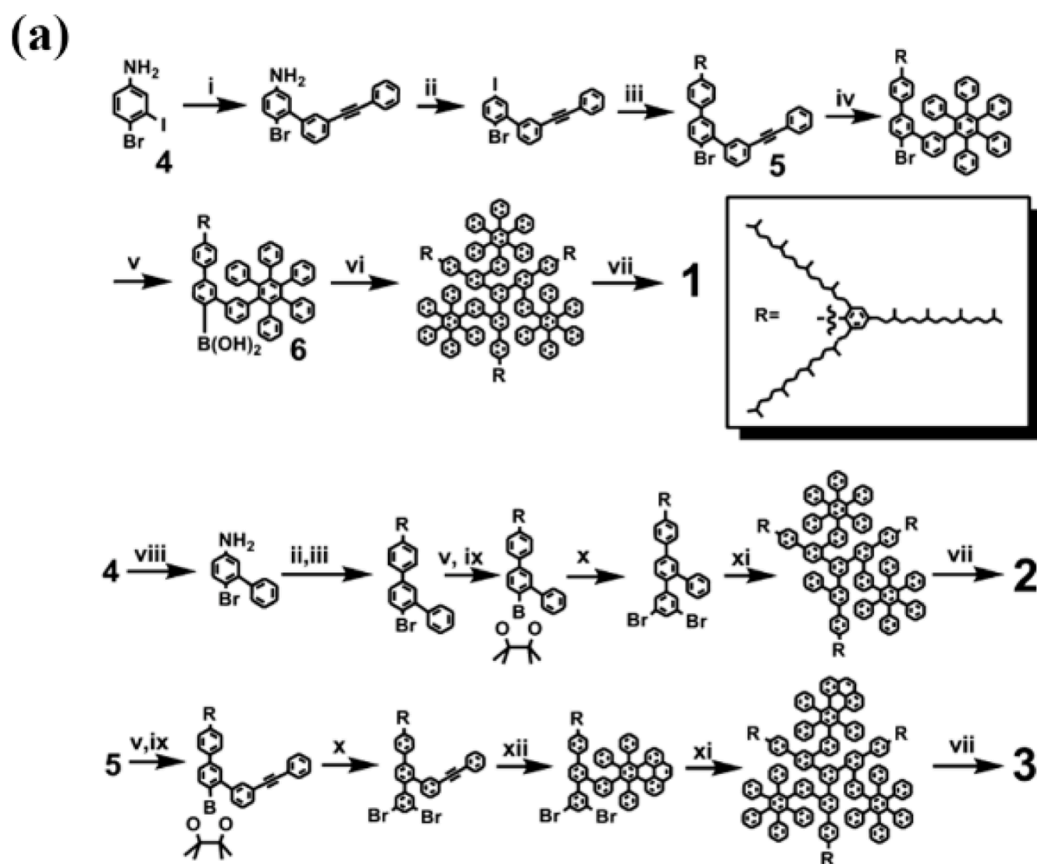


Fig. 7. (a) Synthesis of Graphene Quantum Dots 1–3. Reproduced with permission (Yan et al., 2010). (b) Synthetic procedure of GQDs from nitration of pyrene. Reproduced with permission (Wang et al., 2014).

GQDs possess excellent optical properties such as bright exciton fluorescence, strong exciton absorption bands extending into the visible region, large molar extinction coefficients and long-term photostability.

Hydrothermal methods employed 1,3,6-trinitropyrene as a feedstock in alkaline solution was carried to synthesize hydroxyl-containing GQDs (Yu et al., 2016). Alkaline hydrothermal conditions promoted the denitration and dehydrogenation of 1,3,6-trinitropyrene. The

subsequent generation of suspended carbon-bonded covalent bonds leads to sp^2 fusion between precursors. This method provides high yields and has the potential to be produced on a large scale. In fact, the preparation of GQDs by solution chemistry is usually long and requires several separations.

Yan et al. (Yan et al., 2018) used benzoic acid (BA) as a carbon source and hydrogen and oxygen as explosive sources to synthesize powdered

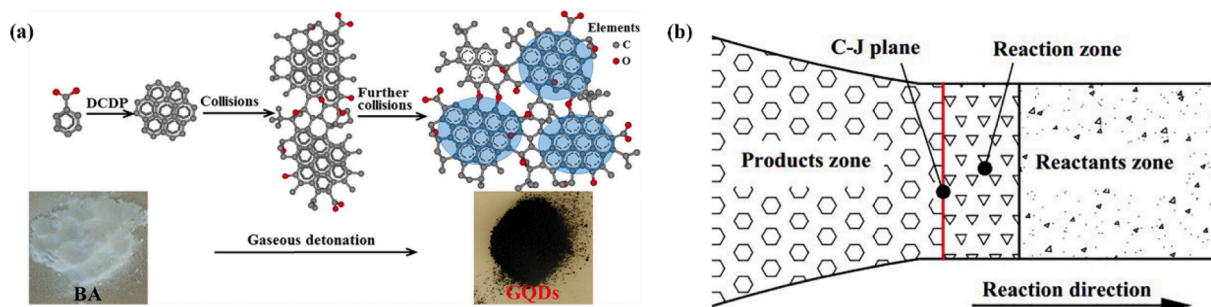
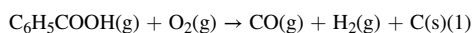


Fig. 8. (a) The preparation and growth mechanism of GQDs. (b) ZND model of detonation. Reproduced with permission (Yan et al., 2018).

GQDs with an average diameter of 2.5 nm in 3–5 ms without any post-treatment using a one-pot gas burst method (Fig. 8a). The results of GQDs were highly reproducible by controlling the detonation parameters. Dispersing the produced GQDs into ethanol resulted in bright blue fluorescence with a quantum yield of 21.5 % when excited under 365 nm UV light. Although it was very difficult to trace and describe the complex reactions, the authors investigated the mechanism of GQDs synthesis by bottom-up method based on their surface structure, PL behavior and gas burst properties. The Zeldovich von Neumann-Döring (ZND) burst model (Fig. 8b) used to explain the formation of GQDs consisted of three regions (reactants, reaction zone and products), where hydrogen reacted with oxygen and generated a large amount of energy.

At the same time, the following reaction occurred due to the excess of oxygen:



This is the source of free carbon. Compared to the GQDs obtained by the bottom-up method, more intermediate sp^3 carbonates are generated during the detonation process at higher temperatures and pressures. According to the C-J (Chapman Jouguet) theory, the temperature and pressure of detonation chemical reactions are higher than 1500 K and 3 MPa, which are more conducive to graphitization. Further, high temperature is conducive to many single step single molecule reactions, including C–H bond breakage and intramolecular rearrangement, while high pressure is conducive to the ordered arrangement of freshly formed C=C and the growth of crystal GQDs.

Norepinephrine molecules (1-(3,4-dihydroxyphenyl)-2-aminoethanol) with redox activity can be fused to form element-doped GQDs under microwave irradiation (Fig. 9a) (Jeon et al., 2016). Salicylic acid (2-hydroxybenzoic acid, also called o-hydroxybenzoic acid) generates aromatic radicals under UV irradiation and then fuses to GQDs with 86 % yield with only H_2O and CO_2 , which is expected to be a new, green, rapid and versatile preparation method (Zhu et al., 2017). Another strategy is that organic molecules or materials can be carbonized into graphitized materials for subsequent exfoliation into GQDs under high temperature and inert atmosphere (Fig. 9b,c). The advantage of this strategy is that it is easy to inherit organic precursors and thus achieve doping of multiple heteroatoms. For example, Ananthanarayanan et al.

(Ananthanarayanan et al., 2015) used the biomolecule ATP as a precursor and could obtain N, P co-doped GQDs with two-photon up conversion properties (Fig. 9e).

Green fluorescent N-doped CQD (N-CQD) with quantum yield of 30.6 % were prepared by a simple bottom-up electrochemical method using a mixture of catechol and ethylenediamine as precursors and electrolytes (Fig. 9d) (Niu et al., 2018). Based on the on and off signals induced by the decomposition and repolymerization of N-CQD. Pyrophosphate anions (PPI) was simultaneously used as a substrate for alkaline phosphatase (ALP) activity assessment. Under optimized conditions, sensitive and specific quantification of Fe^{3+} and PPI and the monitoring of ALP activity were achieved accordingly.

In the preparation of GQDs from phenyl molecules, the number of carbon atoms of quantum dots can be controlled by solution chemistry, and the products have good water solubility, but the preparation of the precursor is complicated and requires precise control of the reaction conditions; Although the products have the defect of low crystallinity, GQDs with high quantum yields can be prepared quickly and efficiently when the quantum dots are synthesized by microwave, UV irradiation or explosion. It is expected to be applied to the large-scale production of powdered GQDs.

4.2. Glucose and citric acid as raw materials

As raw materials, glucose and citric acid are cheap and easy to obtain the green and low-cost GQDs without complicated processing.

Bayat et al. (Bayat and Saievar-Iranizad, 2017) synthesized monolayer GQDs with an average size of 8 nm, good solubility in water and green fluorescence by dissolving glucose in water at 200 °C. During the synthesis process, hydrogen atoms of glucose molecules interact with hydroxyl groups in adjacent glucose molecules to dehydrate, while carbon atoms interact with each other to form C=C, namely the basic unit of GQDs. The final monolayer GQDs are formed (Fig. 10a).

Citric acid is also often used for the preparation of graphene quantum dots by high-temperature pyrolysis. Wang et al. (Wang et al., 2015) used citric acid as a raw material to prepare GQDs with wide size distribution and excitation of blue fluorescence by varying the carbonization temperature and carbonization time (Fig. 10d). The dehydration of citric acid molecules at 180–270 °C formed multimers, which further formed

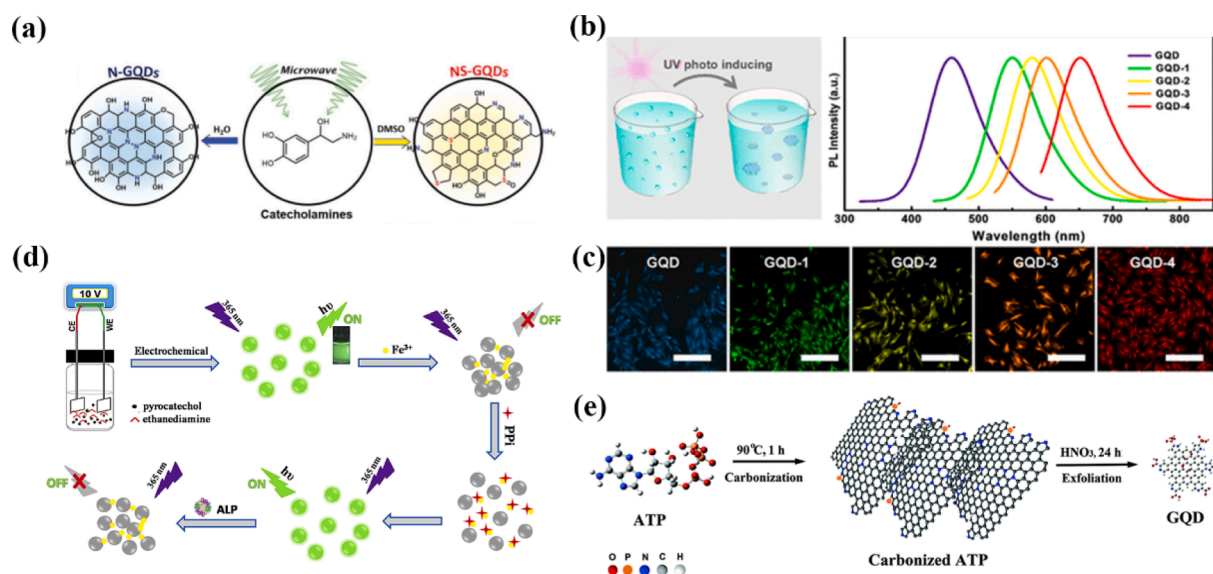


Fig. 9. (a) Schematic illustration of the microwave-assisted synthesis of N-GQDs and NS-GQDs from a single precursor. Reproduced with permission (Jeon et al., 2016). (b) Schematic diagram showing the synthesis progress of GQDs. And the PL spectra of GQD, GQD-1, GQD-2, GQD-3 and GQD-4. (c) Fluorescent microphotograph (scale bar: 5 μm) of OCM-1 cells incubated with GQD, GQD-1, GQD-2, GQD-3 and GQD-4. Reproduced with permission (Zhu et al., 2017). (d) Schematic illustration of the N-CQDs synthesis and the detection strategies for PPI and ALP activity based on the aggregation and disaggregation of the N-CQDs. Reproduced with permission (Niu et al., 2018). (e) Illustration of the synthesis procedure for ATP-GQDs. Reproduced with permission (Ananthanarayanan et al., 2015).

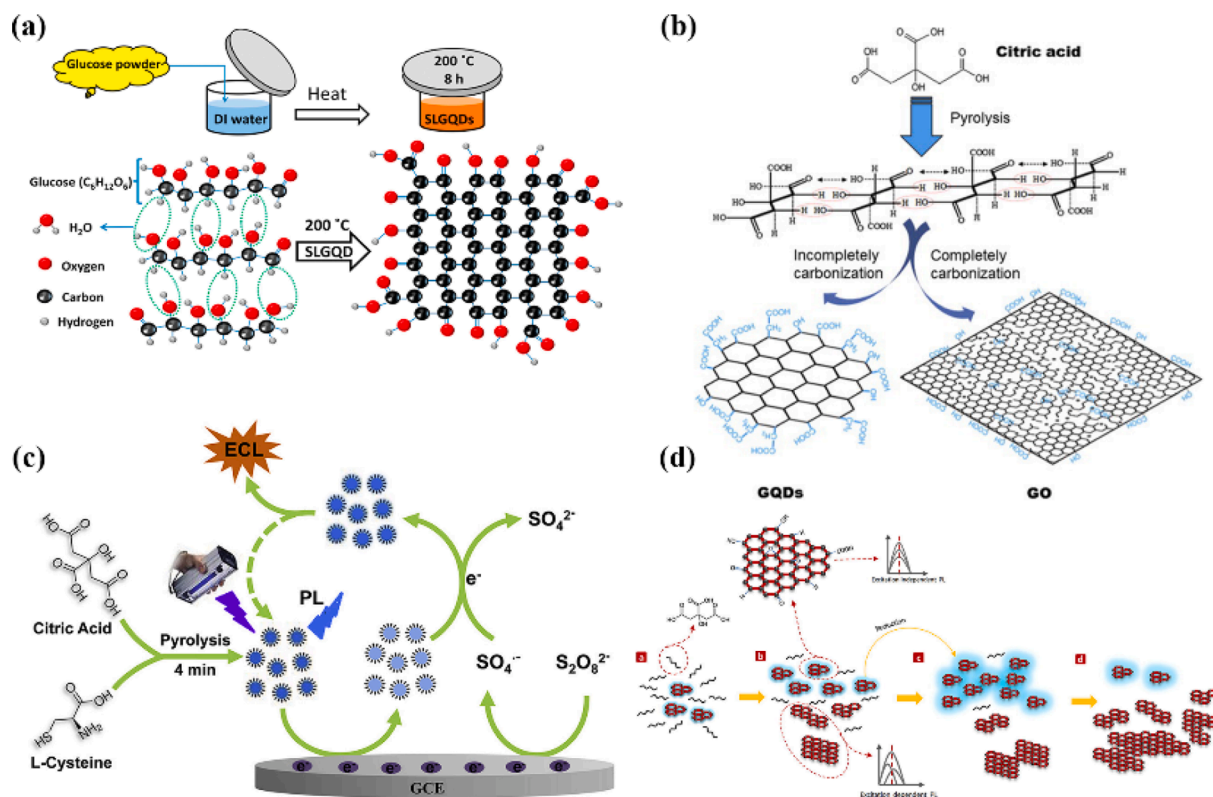


Fig. 10. (a) Formation mechanism of the SLGQDs via a hydrothermal method at 200 °C for 8 h. Reproduced with permission (Bayat and Saievar-Iranizad, 2017). (b) Diagram for the synthesis of GQDs and GO. Reproduced with permission (Dong et al., 2012). (c) Schematic illustration of the NS-GQDs synthesis and the ECL and electron transfer mechanism. Reproduced with permission (Zhang et al., 2018). (d) Schematic representation of the thermal decomposition process of CA. Reproduced with permission (Wang et al., 2015).

small-sized GQDs, and more citric acid was consumed as the heating time increased. The resulting quantum dots are rich in negatively charged functional groups such as carboxyl and hydroxyl groups at the edges, and the interaction between these functional groups and cations affects the photoluminescence of quantum dots. In-depth studies have shown that Fe^{3+} has a strong fluorescence quenching effect on the quantum dots made from citric acid, so they can be used for Fe^{3+} detection. Dong et al. (Dong et al., 2012) produced small-sized graphene quantum dots by partial carbonization of citric acid and larger-sized graphene oxide by complete carbonization of citric acid (Fig. 10b). Hong et al. (Hong et al., 2018) prepared GQDs by pyrolysis of trisodium citrate (Fig. 11a), and then obtained monolayer GQDs with the lateral size of only 1.3 ± 0.5 nm by ultrafiltration. Zhang et al. (Zhang et al., 2018) synthesized nitrogen and sulfur co-doped GQDs by a facile pyrolysis method using citric acid and L-cysteine as precursors (Fig. 10c). Gu et al. (Gu et al., 2020) obtained highly amidated GQDs by pyrolysis of citric acid and urea at 250 °C for 0.5 h with IR assistance. These graphene quantum dots can be used as nonmetallic electrocatalysts for electrochemical hydrogen adsorption and oxygen reduction reactions in acidic and alkaline electrolytes. It can be seen that the citric acid-based precursor pyrolysis method can provide precise control of the GQDs size while retaining the heteroatoms in the precursor molecules to achieve the modification of GQDs.

Citric acid has also been used in the hydrothermal method for the preparation of GQDs (Malahom et al., 2023); Jarujamrus et al. reported that citric acid and tris(hydroxymethyl)aminomethane were precursors for the one-step synthesis of N-GQDs via in situ hydrothermal methods (Fig. 11b), providing a high quantum yield of 57.9 %. Specifically, the fluorescence of N-GQDs is quenched by the incorporation of Ag^+ via a photoinduced electron transfer (PET). Notably, the developed sensor has advantages in terms of simplicity, rapidity, low cost, and high selectivity toward CN^- .

4.3. Amino acids as raw materials

Amino acids, as the basic unit for protein synthesis by living organisms, contain heteroatoms such as oxygen and nitrogen in addition to carbon, which are ideal raw materials for the rapid preparation of GQDs.

Nafiujjaman et al. (Nafiujjaman et al., 2018) used L-glutamic acid as raw material and synthesized BGQDs with an average size of 20 nm and a quantum yield of 24 % by pyrolysis at 220 °C. The effect of BGQDs on the hemolysis rate and morphology of erythrocytes was investigated by mixing different concentrations of BGQDs solutions with human blood, and the results showed that the hemolysis rate of erythrocytes was as low as 0.9 %, which indicates that the obtained BGQDs have good biocompatibility. Zhang et al. (Zhang et al., 2016) prepared GQDs with good water solubility by microwave-assisted pyrolysis using aspartic acid and ammonium bicarbonate as raw materials; The average size of the prepared GQDs was 2.1 nm, and the blue fluorescence could be excited with a quantum yield of 14 %. After adding them to the cell culture medium, a clear blue fluorescence could be observed in the cells under 405 nm excitation and the cell activity was not significantly affected. When it was used for Fe^{3+} detection, the fluorescence quenching rate had a good linear relationship with Fe^{3+} concentration and a wide detection range.

The preparation of GQDs from amino acids by pyrolysis requires less instrumentation and the preparation process is simple. In addition, the amino acids used are usually α -amino acids, which are the basic units for protein synthesis, so the above GQDs have certain nitrogen doping and good biocompatibility, and are less toxic to cells, which have a greater potential for bioimaging applications.

As can be seen, the usual pyrolysis or hydrothermal/solventothermal methods for the preparation of GQDs when organic small molecules are used as precursors require the use of a heating device, which may lead to inhomogeneous GQDs size due to uneven heating inside the heating

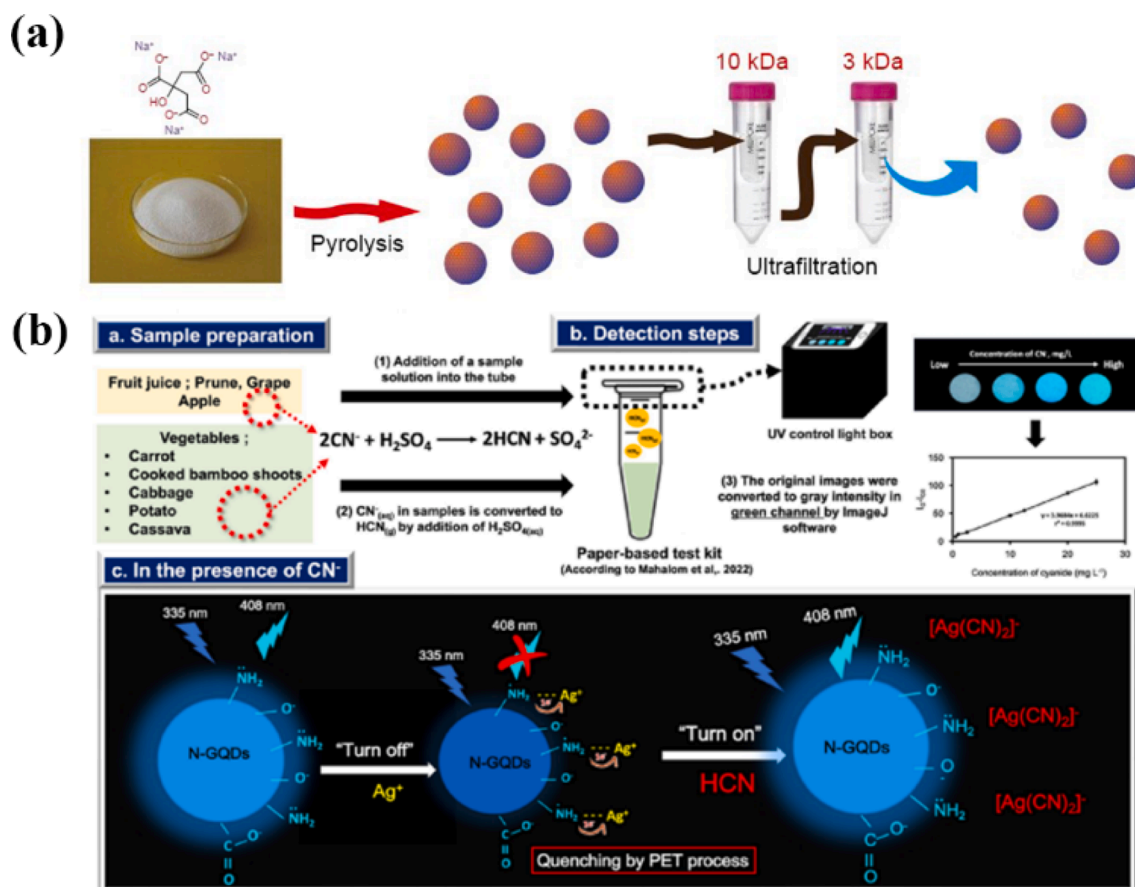


Fig. 11. (a) Processing diagram for the preparation of photoluminescent GQDs. Reproduced with permission (Hong et al., 2018). (b) Diagram illustrating the procedure and working principle of the fluorometric paper-based test kit for cyanide determination based on N-GQDs. Reproduced with permission (Malahom et al., 2023).

device. The microwave method provides a uniform and fast heating method to prepare uniformly sized and distributed graphene quantum dots. However, the hydrothermal/solventothermal method is convenient for the preparation and tuning of heteroatom-doped graphene quantum dots and has advantages in the study of their photoluminescence behavior.

5. Others as raw materials

Fullerene (C_{60}) is a spherical or ellipsoidal all-carbon material with a structure more similar to graphene. If the conditions of the fullerene open-cage reaction can be precisely controlled, uniform-sized GQDs can be obtained. As shown in Fig. 12, Lu et al. (Lu et al., 2011) used the strong interaction between C_{60} and ruthenium to form vacancies and embed C_{60} molecules on the surface of single-crystal ruthenium catalysts, and the embedded molecules fragmented at high temperatures to form carbon clusters, followed by further diffusion and aggregation to form regularized GQDs. By controlling and optimizing the annealing temperature and the density of carbon clusters, GQDs with well-defined geometry could be assembled from C_{60} -derived carbon clusters. Chen et al. (Chen et al., 2020) treated fullerenes under acid-free condition, and offered a convenient proposal to obtain uniform blue-green emissive GQDs and modified efficient orange-emitting graphene quantum dots (D-GQDs) (Fig. 13b). The as-prepared D-GQDs demonstrate remarkable conversion efficiency which quantum yield is up to 52.4 % with the emission peak of 617 nm. Also, GQDs and D-GQDs were blended with poly(vinyl alcohol) (PVA) to prepare transparent photo-luminescent films, which show excellent flexibility and preferable white emission property meeting the requirements of commercial white LEDs.

Carbon nanotubes are often regarded as coiled graphene and are an ideal raw material for the preparation of structurally regular GQDs. Danilov et al. (Danilov et al., 2021) prepared GQDs with 1.5–3 nm in size and a blue emission from electrochemically synthesized partially unzipped multi-walled carbon nanotubes ultrasonically treated for one hour. GQDs served as an active layer to fabricate oxygen electrodes were carried out in a fuel half-cell with an alkaline electrolyte. The fabricated oxygen electrodes were stable for six months at a discharge current density of 200 mA cm^{-2} . The obtained GQDs are promising materials as a new type of catalyst carriers for oxygen electrodes of fuel cells. Iannazzo et al. (Iannazzo et al., 2018) reacted multi-walled carbon nanotubes with mixed acid (concentrated nitric acid and sulfuric acid) solution, and the surface of the graphene quantum dots synthesized by acid exfoliation was rich in oxygen-containing functional groups (Fig. 13a). However, the removal of the strong acid after the reaction increased the cost of the synthesis due to the high concentration of strong acid used in the synthesis process.

In recent years, it has been also seen that the rise of research on the preparation of GQDs from environmentally friendly biomass-carbonaceous waste. The preparation of GQDs from such raw materials has the advantages of being sustainable, renewable, low toxicity and green. Lignin, as one of the main components of woody fiber biomass feedstock, is the most abundant natural aromatic polymer in nature and has unique advantages. Xu et al. (Xu et al., 2019) synthesized GQDs with multiple functional groups by a two-step process of oxidative cleavage and sp^2 hybridization using lignin sulfonate as a feedstock. Ding et al. (Ding et al., 2016) synthesized nitroxylated functionalized single-crystal GQDs with high quantum yield, bright fluorescence, upconversion functionality and long-term stability using alkali lignin

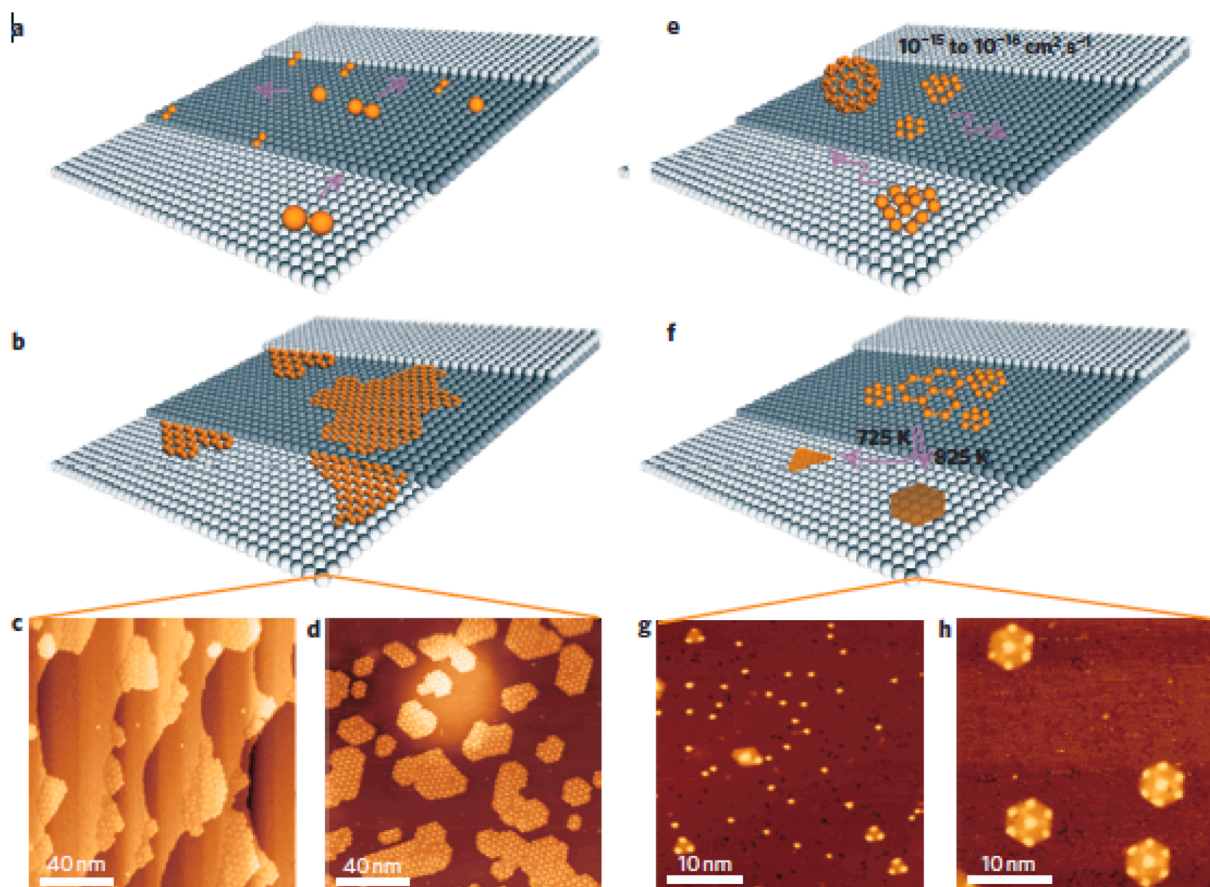


Fig. 12. Comparison of the growth mechanism of graphene nanoislands and quantum dots using C_2H_4 and C_{60} . a-d, Mechanisms using C_2H_4 . e-h, Mechanisms using C_{60} . Reproduced with permission (Lu et al., 2011).

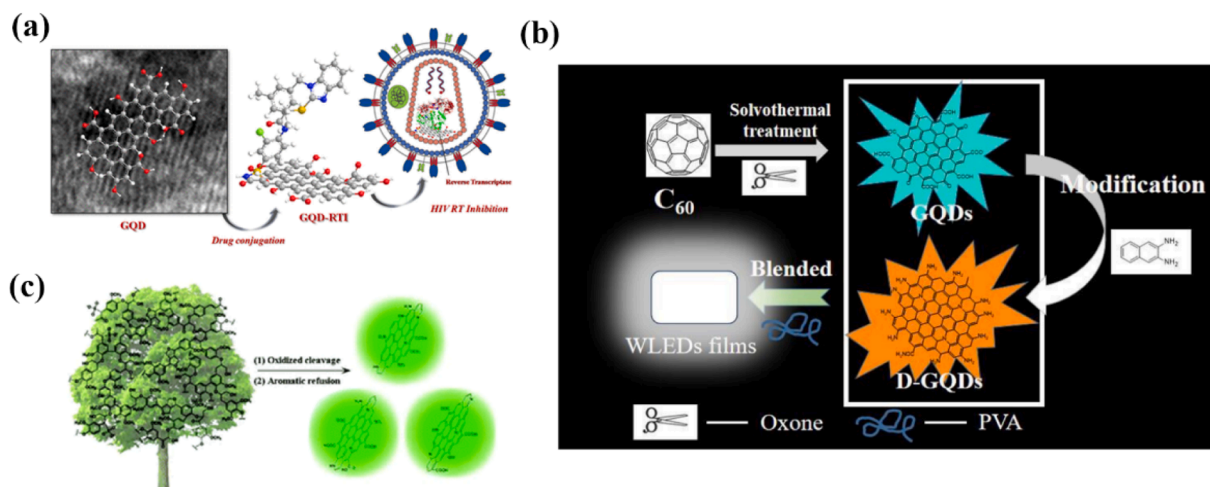


Fig. 13. (a) Schematic illustration of the mechanism using graphene Quantum Dots as HIV Inhibitors. Reproduced with permission (Iannazzo et al., 2018). (b) Schematic preparation process of luminescent composite film based on GQDs and D-GQDs. Reproduced with permission (Chen et al., 2020). (c) The synthesis of single-crystalline graphene quantum dots derived from biomass waste. Reproduced with permission (Ding et al., 2016).

(Fig. 13c).

Han Wei et al. (Han et al., 2021) synthesized nitrogen and sulfur double-doped graphene quantum dots (N, S-GQDs) from aqueous soy protein-citric acid-urea solutions by a hydrothermal method. It is worth mentioning that the ethanol precipitation kettle-liquid separation method used in this study provides rapid access to N, S-GQDs solids, offering the possibility of mass production of biomass graphene

quantum dots.

Waste biomass such as sugarcane bagasse (Chai et al., 2019), waste leather scraps, and coffee grounds (Kim et al., 2021) (Fig. 14) are also gradually developed as raw materials for the synthesis of GQDs with good water solubility and excellent optical properties, realizing the effective utilization of solid waste.

Currently, fullerenes and carbon nanotubes can be used as raw

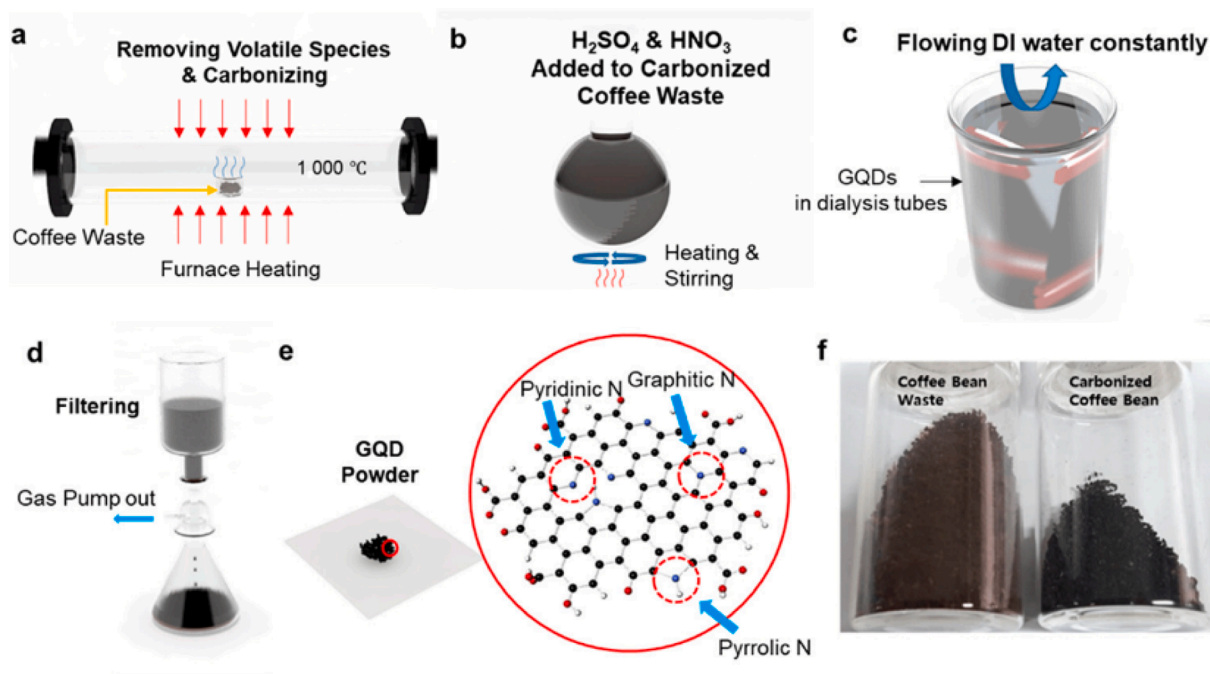


Fig. 14. Schematic illustration of the synthesis of coffee bean-derived GQDs. Reproduced with permission (Kim et al., 2021).

materials to produce GQDs with uniform size and good performance, but fullerenes are expensive and carbon nanotubes are prepared under harsh conditions, so it is difficult to use them for large-scale fabrication of high-quality GQDs. Studies on the preparation of quantum dots from lignin generally use a more complicated two-step method or use strong acids such as sulfuric acid or nitric acid in the preparation process.

The raw materials and methods applied to fabricate GQDs affect the size and quantum yield of the obtained GQDs. At present, the impact pattern is not yet clear. The following Table 1 lists some representative situation.

6. Conclusion and outlook

The performance of GQDs depends on both the synthesis process and the raw materials used. In here, we have mainly reviewed the preparation of GQDs from different raw materials. The commonly used raw materials are graphite, coal and coke, and organic small molecules such as citric acid and amino acids, etc. The properties of GQDs obtained from each type of raw materials differ depending on their structures and properties, and the applicable preparation methods.

Due to the large size of graphite particles, only micrometer sized graphite flakes can be obtained after strong acid oxidation, ultrasonic peeling, chemical reduction and other steps. Therefore, people have attempted to further cut two-dimensional graphite flakes using methods such as chemical ablation, microwave ablation, and electrochemical oxidation. The diameter distribution of GQDs obtained by this method is extremely uneven, requiring complex separation processes such as filtration and dialysis to obtain more uniform GQDs, resulting in lower product yield and quantum yield. Here, we recommend that graphitized precursors such as graphite, graphene and coke with high degree of graphitization can be used to prepare high quality GQDs by electrolysis method due to their good electrical conductivity, avoiding the use of strong acids and strong oxidants, and preparing quantum dots with better size uniformity and higher quantum yields. Based on the great flexibility of the conjugated carbon skeleton, the GQDs facilitate the construction of complex and conductive architectures, which can be used in photovoltaic conversion devices to improve the conversion efficiency.

Graphene oxide is rich in oxygen-containing functional groups, which can be easily cleaved by strong oxidizing agents under hydrothermal or solvothermal conditions or by reducing agents to break the C-O bonds on the epoxy groups, and the size of the resulting GQDs depends on the abundance of epoxy groups on the precursors. Among this process, oxidation cutting can enhance the edge structure and functional groups of GQDs and thus provide a large number of active sites, which is convenient for chemical energy storage applications; The GQDs generated by reduction fragmentation contain a small number of oxygen-containing groups and defects, and they are smaller in size and have higher quantum yields, which can better exploit their fluorescence properties. However, the amount of strong acids and oxidants used in the preparation process is large, and additional reagents must be applied to neutralize them during the post-treatment; Meanwhile, the time consuming separation and purification in the preparation of GO reduces its preparation efficiency.

Coal contains nanoscale graphitized carbon structure, which leads to a more fragile connection of amorphous carbon. Therefore, we suggest ultrasonic stripping (cleavage) method to obtain GQDs from coal, which is both efficient and relatively environmentally friendly, but the specific process conditions still need to be further explored and optimized. Coal and carbon black are relatively low cost and more promising for application in large-scale industrial GQDs production.

In contrast, GQDs are generally synthesized from organic small molecules such as citric acid, glucose and amino acids through multi-step synthesis, pyrolysis reaction, or polymerization reaction. This method can design the structure and function of GQDs at the atomic level, and is expected to have great development in the future especially in metal ion detection and bioimaging due to their better water solubility and biocompatibility.

If GQDs are applied in the fields of biological imaging and drug delivery, we recommend using foodborne biomass as raw materials to prepare GQDs, or if precise regulation is required, organic small molecules as raw materials is recommended. Although several methods and raw materials have been developed for the preparation of GQDs, there are still many challenges:

Table 1
Comparison of Graphene Quantum Dots Synthesized from Varied Raw Materials.

Raw materials	Method	Average size (nm)	Quantum yield	Functional group	Related literature
graphite rods	Electrolysis; Reduction	5–10	14 %	hydrazide	(Zhang et al., 2012)
graphene films	Electrolysis	3–5	—	O-rich	(Li et al., 2011)
foam-like 3D graphene	Electrolysis	~3	~10 %	—	(Ananthanarayanan et al., 2014)
GO powder	Oxidation	2–4; 3–5	34.8 %	—	(Shi et al., 2023; Fan et al., 2015)
graphene oxide (GO)	Solvent heat	2–3	—	—	(Fan et al., 2023)
	Hydro-thermal method	1.5–3	—	—	(Zhang et al., 2022)
	Hydrothermal method.	20–50	—	—	(Kharangarh et al., 2022)
nanoscale GOs	Hydrothermal treatment	—	18.2 %	—	(Wu et al., 2016)
monolayers of GO	Thermal reduction; Oxidation; Hydrothermal treatment	1.5–5	—	carboxyl groups	(Pan et al., 2012)
bituminous coal	Liquid phase oxidation	3.2	—	carbonyl group	(Zhu et al., 2022)
bituminous coal	Heat treated; Oxidation; Solvent heat	2.5–5	14.42 %	—	(Ghorai et al., 2018)
anthracite powder	Ultrasonic treatment	2.2–4.2	5.98 %	—	(Zhang et al., 2019)
coke	One-step electrolytic stripping	3–4.6	9.24 %	Alkenyl group; carbonyl group	(He et al., 2018)
coal tar pitch	Heating with high carbon content	1.3–2.1	80 %	—	(Liu et al., 2018)
benzoic acid	Gaseous detonation	1.5–3.9	5.25 %	—	(Yan et al., 2018)
glucose	One-step hydro-thermal	~8	—	—	(Bayat and Saievar-Iranizad, 2017)
Pyrene (C ₁₆ H ₁₀)	Water-phase molecular fusion	1.4–4.7	—	Hydroxyl	(Wang et al., 2014)
Oxygen containing aromatic compounds	Free radical polymerization	1.5–4.5	86 %	—	(Zhu et al., 2017)
Citric acid (CA)	directly pyrolyzing	15	2.2 %	Hydroxyl group; Ether group	(Dong et al., 2012)
trisodium citrate	Pyrolysis	0.8–1.8	—	Oxygen-containing group	(Hong et al., 2018)
L-glutamic acid	Pyrolysis	20–40	24 %	—	(Nafujjaman et al., 2018)
aspartic acid ammonium bicarbonate	Microwave-assisted pyrolysis	0.3–4	14 %	C=O and C-OH/C-O-C group	(Zhang et al., 2016)
cellulose	Hydrothermal synthesis	—	—	carboxyl group	(Mahalingam et al., 2023)
C ₆₀	High temperature fragmentation acid-free condition	< 5 nm	30 ± 2 %	—	(Lu et al., 2011)
unzipped multi-walled carbon nanotubes	ultrasonically treated	2–4.5 nm	52.4 %	C=O/C—N	(Chen et al., 2020)
	ultrasonically treated	1.5–3 nm	—	C=O/COOH	(Danilov et al., 2021)
alkali lignin	oxidative cleavage and aromatic refusion	~3.7 nm	21 %	nitroxylated functionalized	(Ding et al., 2016)
soy protein	hydrothermal method	2–5 nm	9.23 %	nitrogen and sulfur double-doped	(Han et al., 2021)
sugarcane bagasse	hot-water pretreatment	2.26 nm	—	C=O	(Chai et al., 2019)
coffee grounds	chemical vapor deposition/ thermo-oxidative cutting	2.6–3.69 nm	—	C—N carboxyl groups	(Kim et al., 2021)

- (1) How to precisely regulate the size of GQDs and control the GQDs morphology and edge functional groups by controlling the reaction conditions.
- (2) Development of controllable, efficient, environmentally friendly and suitable methods for large-scale synthesis of GQDs.
- (3) The development of highly targeted and selective methods for the synthesis of GQDs requires continued exploration.

Due to the non-stoichiometric nature of GQDs, the specific control of their optical properties and their practical applications have become a challenging issue. There are many factors that affect the fluorescence luminescence performance of GQDs. For example, synthesis methods, size, pH value, surface chemical functional groups, reaction solvents, heteroatom doping, and surface defects.

The preparation and application research of GQDs are still in the laboratory design stage, and how to develop low-cost and green technologies to prepare GQDs with high chemical stability, high fluorescence quantum yield, stable and controllable morphological size, and functionalize groups on the surface through rational selection of raw materials and optimization of preparation methods and processes is the key issue for developing their application research and industrialization.

Declaration of competing interest

The authors declare that they have no known competing financial interests or personal relationships that could have appeared to influence the work reported in this paper.

Acknowledgement

This research is supported by Key Program (U20A20235) funded by National Natural Science Foundation of China, The National Natural Science Foundation of China (52171127, 51974242), Regional Innovation Capability Guidance Program of Shaanxi Provincial Government (2022QFY10-06), and Key R&D Program of Xianyang Science and Technology Bureau (2021ZDYF-GY-0029).

References

- Ahirwar, S., Mallick, S., Bahadur, D., 2017. Electrochemical method to prepare graphene quantum dots and graphene oxide quantum dots. *ACS Omega*. 2, 8343–8353. <https://doi.org/10.1021/acsomega.7b01539>.
- Ananthanarayanan, A., Wang, X., Routh, P., Sana, B., Lim, S., Kim, D.-H., Lim, K.-H., Li, J., Chen, P., 2014. Facile synthesis of graphene quantum dots from 3D graphene

- and their application for Fe³⁺ sensing. *Adv. Funct. Mater.* 24, 3021–3026. <https://doi.org/10.1002/adfm.201303441>.
- Ananthanarayanan, A., Wang, Y., Routh, P., Sk, M.A., Than, A., Lin, M., Zhang, J., Chen, J., Sun, H., Chen, P., 2015. Nitrogen and phosphorus co-doped graphene quantum dots: synthesis from adenosine triphosphate, optical properties, and cellular imaging. *Nanoscale* 7, 8159–8165. <https://doi.org/10.1039/C5NR01519G>.
- Bayat, A., Saievar-Iranizad, E., 2017. Synthesis of green-photoluminescent single layer graphene quantum dots: determination of HOMO and LUMO energy states. *J. Lumin.* 192, 180–183. <https://doi.org/10.1016/j.jlumin.2017.06.055>.
- Carrasco, P.M., García, I., Yate, L., Tena Zaera, R., Cabañero, G., Grande, H.J., Ruiz, V., 2016. Graphene quantum dot membranes as fluorescent sensing platforms for Cr (VI) detection. *Carbon* 109, 658–665. <https://doi.org/10.1016/j.carbon.2016.08.038>.
- Chai, X., He, H., Fan, H., Kang, X., Song, X., 2019. A hydrothermal-carbonization process for simultaneously production of sugars, graphene quantum dots, and porous carbon from sugarcane bagasse. *Bioresour. Technol.* 282, 142–217. <https://doi.org/10.1016/j.biortech.2019.02.126>.
- Chang, Y.-H., Chang, C.-C., Chang, L.-Y., Wang, P.-C., Kanokpaka, P., Yeh, M.-H., 2023. Self-powered triboelectric sensor with N-doped graphene quantum dots decorated polyaniline layer for non-invasive glucose monitoring in human sweat. *Nano Energy* 112, 108505 <https://doi.org/10.1016/j.nanoen.2023.108505>.
- Chen, Y.-X., Lu, D., Wang, G.-G., Huangfu, J., Wu, Q.-B., Wang, X.-F., Liu, L.-F., Ye, D.-M., Yan, B., Han, J., 2020. Highly efficient orange emissive graphene quantum dots prepared by acid-free method for white LEDs. *ACS Sustain. Chem. Eng.* 8, 6657–6666. <https://doi.org/10.1021/acssuschemeng.0c00106>.
- Chen, J., Yao, B., Li, C., Shi, G., 2013. An improved hummers method for eco-friendly synthesis of graphene oxide. *Carbon* 64, 225–229. <https://doi.org/10.1016/j.carbon.2013.07.055>.
- Chung, S., Revia, R.A., Zhang, M., 2021. Graphene quantum dots and their applications in bioimaging, biosensing, and therapy. *Adv. Mater.* 33, 1904362 <https://doi.org/10.1002/adma.201904362>.
- Danilov, M.O., Pomanuk, S.S., Dovbeshko, G.I., Gnatyuk, O.P., Rusetskiy, I.A., Kolbasov, G.Y., 2021. Graphene quantum dots from partially unzipped multi-walled carbon nanotubes: promising materials for oxygen electrodes. *J. Electrochem. Soc.* 168, 044514 <https://doi.org/10.1149/1945-7111/abf4b3>.
- Ding, Z., Li, F., Wen, J., Wang, X., Sun, R., 2016. Gram-scale synthesis of single-crystalline graphene quantum dots derived from lignin biomass. *Green Chem.* 20, 1383–1390. <https://doi.org/10.1039/C7CG03218H>.
- Dong, Y., Shao, J., Chen, C., Li, H., Wang, R., Chi, Y., Lin, X., Chen, G., 2012. Blue luminescent graphene quantum dots and graphene oxide prepared by tuning the carbonization degree of citric acid. *Carbon* 50, 4738–4743. <https://doi.org/10.1016/j.carbon.2012.06.002>.
- Fan, M., Wang, Z., Sun, K., Wang, A., Zhao, Y., Yuan, Q., Wang, R., Raj, J., Wu, J., Jiang, J., Wang, L., 2023. N-B-OH site-activated graphene quantum dots for boosting electrochemical hydrogen peroxide production. *Adv. Mater.* 35, 2209086 <https://doi.org/10.1002/adma.202209086>.
- Fan, C., Yang, R., Huang, Y., Mao, L., Yang, Y., Gong, L., Dong, X., Yan, Y., Zou, Y., Zhong, L., Xu, Y., 2023. Graphene quantum dots as sulfiphilic and lithiophilic mediator toward high stability and durable life lithium-sulfur batteries. *J. Energy Chem.* <https://doi.org/10.1016/j.jechem.2023.06.030>.
- Fan, T., Zeng, W., Tang, W., Yuan, C., Tong, S., Cai, K., Liu, Y., Huang, W., Min, Y., Epstein, A.J., 2015. Controllable size-selective method to prepare graphene quantum dots from graphene oxide. *Nanoscale Res. Lett.* 10, 55. <https://doi.org/10.1186/s11671-015-0783-9>.
- Ghorai, S., Roy, I., De, S., Dash, P.S., Basu, A., Chattopadhyay, D., 2018. Exploration of the potential efficacy of natural resource-derived blue-emitting graphene quantum dots in cancer therapeutic applications. *New J. Chem.* 44, 5366–5376. <https://doi.org/10.1039/C9NJ06239D>.
- Gu, S., Hsieh, C.-T., Mallick, B.C., Gandomi Ashraf, Y., 2020. Infrared-assisted synthesis of highly amidized graphene quantum dots as metal-free electrochemical catalysts. *Electrochim. Acta* 360, 137009 <https://doi.org/10.1016/j.electacta.2020.137009>.
- Ham, Y., Kim, C., Shin, D., Kim, I., Kang, K., Jung, Y., Lee, D., Jeon, S., 2023. All-graphene quantum dot-derived battery: Regulating redox activity through localized subdomains. *Small* 2303432. <https://doi.org/10.1002/sml.202303432>.
- Han, W., Zhan, J., Shi, H., Zhao, D., Cai, S., Peng, X., Xiao, B., Gao, Y., 2021. Synthesis and properties of nitrogen and sulfur codoped graphene quantum dots. *CIESC J.* 72, 530–538. <https://doi.org/10.11949/0438-1157.20200997>.
- Han, W., Lee, H., Liu, Y., Kim, Y., Chu, H., Liu, G., Yang, W., 2023. Toward highly reversible aqueous zinc-ion batteries: nanoscale-regulated zinc nucleation via graphene quantum dots functionalized with multiple functional groups. *Chem. Eng. J.* 452, 139090 <https://doi.org/10.1016/j.cej.2022.139090>.
- He, M., Guo, X., Huang, J., Shen, H., Zeng, Q., Wang, L., 2018. Mass production of tunable multicolor graphene quantum dots from an energy resource of coke by a one-step electrochemical exfoliation. *Carbon* 140, 508–520. <https://doi.org/10.1016/j.carbon.2018.08.067>.
- Hong, G.-L., Zhao, H.-L., Deng, H.-H., Yang, H.-J., Peng, H.-P., Liu, Y.-H., Chen, W., 2018. Fabrication of ultra-small monolayer graphene quantum dots by pyrolysis of trisodium citrate for fluorescent cell imaging. *Int. J. Nanomed.* 13, 4807–4815. <https://doi.org/10.2147/IJN.S168570>.
- Hsieh, C.-T., Sung, P.-Y., Gandomi, Y.A., Khoo, K.S., Chang, J.-K., 2023. Microwave synthesis of boron- and nitrogen-codoped graphene quantum dots and their detection to pesticides and metal ions. *Chemosphere* 318, 137926. <https://doi.org/10.1016/j.chemosphere.2023.137926>.
- Iannazzo, D., Pistone, A., Ferro, S., De Luca, L., Monforte, A.M., Romeo, R., Buemi, M.R., Pannecouque, C., 2018. Graphene quantum dots based systems as HIV inhibitors. *Bioconjugate Chem.* 29, 3084–3093. <https://doi.org/10.1021/acs.bioconjchem.8b00448>.
- Jeon, S., Kang, T., Ju, J., Kim, M., Park, J.H., Raza, F., Han, J., Lee, H., Kim, J., 2016. Modulating the photocatalytic activity of graphene quantum dots via atomic tailoring for highly enhanced photocatalysis under visible light. *Adv. Funct. Mater.* 26, 8211–8219. <https://doi.org/10.1002/adfm.201603803>.
- Kharangarh, P.R., Singh, G., 2023. Effect of Mo-doped strontium cobaltite on graphene nanosheets for creating a superior electrode in supercapacitor applications. *ECS J. Solid State Sci. Technol.* 12, 031006 <https://doi.org/10.1149/2162-8777/acc095>.
- Kharangarh, P.R., Umopathy, S., Singh, G., 2018. Investigation of sulfur related defects in graphene quantum dots for tuning photoluminescence and high quantum yield. *Appl. Surf. Sci.* 449, 363–370. <https://doi.org/10.1016/j.apsusc.2018.01.026>.
- Kharangarh, P.R., Gupta, V., Singh, A., Bhardwaj, P., Grace, A.N., 2020. An efficient pseudocapacitor electrode material with co-doping of iron (II) and sulfur in luminescent graphene quantum dots. *Diamond Relat. Mater.* 107, 107913 <https://doi.org/10.1016/j.diamond.2020.107913>.
- Kharangarh, P.R., Ravindra, N.M., Rawal, R., Singh, A., Gupta, V., 2021. Graphene quantum dots decorated on spinel nickel cobaltite nanocomposites for boosting supercapacitor electrode material performance. *J. Alloys Compd.* 876, 159990 <https://doi.org/10.1016/j.jallcom.2021.159990>.
- Kharangarh, P.R., Ravindra, N.M., Singh, G., Umopathy, S., 2022. Synthesis and characterization of Nb-doped strontium cobaltite@GQD electrodes for high performance supercapacitors. *J. Energy Storage* 55, 105388. <https://doi.org/10.1016/j.est.2022.105388>.
- Kharangarh, P.R., Ravindra, N.M., Singh, G., Umopathy, S., 2023. Synthesis of luminescent graphene quantum dots from biomass waste materials for energy-related applications-An overview. *Energy Storage* 5, e390.
- Kim, D.J., Yoo, J.M., Suh, Y., Kim, D., Kang, I., Moon, J., Park, M., Kim, J., Kang, K.-S., Hong, B.H., 2021. Graphene quantum dots from carbonized coffee bean wastes for biomedical applications. *Nanomaterials* 11, 1423. <https://doi.org/10.3390/nano11061423>.
- Kolhe, P., Roberts, A., Gandhi, S., 2023. Fabrication of an ultrasensitive electrochemical immunosensor coupled with biofunctionalized zero-dimensional graphene quantum dots for rapid detection of cephalixin. *Food Chem.* 398, 133846 <https://doi.org/10.1016/j.foodchem.2022.133846>.
- Kurniawan, D., Anjali, B.A., Setiawan, O., Ostrikov, K.K., Chung, Y.G., Chiang, W.-H., 2022. Microplasma band structure engineering in graphene quantum dots for sensitive and wide-range pH sensing. *ACS Appl. Mater. Interfaces* 14, 1670–1683. <https://doi.org/10.1021/acscami.1c18440>.
- Kurniawan, D., Mathew, J., Rahardja, M.R., Pham, H., Wong, P., Rao, N.V., (Ken) Ostrikov, K., Chiang, W., 2023. Plasma-enabled graphene quantum dot hydrogels as smart anticancer drug nanocarriers. *Nano* 19, 2206813 <https://doi.org/10.1002/sml.202206813>.
- Li, Y., Hu, Y., Zhao, Y., Shi, G., Deng, L., Hou, Y., Qu, L., 2011. An electrochemical avenue to green-luminescent graphene quantum dots as potential electron-acceptors for photovoltaics. *Adv. Mater.* 23, 776–780. <https://doi.org/10.1002/adma.201003819>.
- Li, X., Rui, M., Song, J., Shen, Z., Zeng, H., 2015. Carbon and graphene quantum dots for optoelectronic and energy devices: a review. *Adv. Funct. Mater.* 25, 4929–4947. <https://doi.org/10.1002/adfm.201501250>.
- Liu, R., Yang, R., Qu, C., Mao, H., Hu, Y., Li, J., Qu, L., 2017. Synthesis of glycine-functionalized graphene quantum dots as highly sensitive and selective fluorescent sensor of ascorbic acid in human serum. *Sens. Actuators B Chem.* 241, 644–651. <https://doi.org/10.1016/j.snb.2016.10.096>.
- Liu, Q., Zhang, J., He, H., Huang, G., Xing, B., Jia, J., Zhang, C., 2018. Green preparation of high yield fluorescent graphene quantum dots from coal-tar-pitch by mild oxidation. *Nanomaterials* 8, 844. <https://doi.org/10.3390/nano8100844>.
- Lu, J., Yeo, P.S.E., Gan, C.K., Wu, P., Loh, K.P., 2011. Transforming C₆₀ molecules into graphene quantum dots. *Nat. Nanotechnol.* 6, 247–252. <https://doi.org/10.1038/nnano.2011.30>.
- Mahalingam, S., Manap, A., Rabeya, R., Lau, K.S., Chia, C.H., Abdullah, H., Amin, N., Chelvanathan, P., 2023. Electron transport of chemically treated graphene quantum dots-based dye-sensitized solar cells. *Electrochim. Acta* 439, 141667 <https://doi.org/10.1016/j.electacta.2022.141667>.
- Malahom, N., Ma-In, T., Naksen, P., Anutrasakda, W., Amatongchai, M., Citterio, D., Jarujamrus, P., 2023. Nitrogen-doped graphene quantum dots as “Off-On” fluorescent probes in paper-based test kits for selective monitoring of cyanide in food. *ACS Appl. Nano Mater.* 6, 11144–11153. <https://doi.org/10.1021/acsnanm.3c01109>.
- Martins, E.C., Santana, E.R., Spinelli, A., 2023. Nitrogen and sulfur co-doped graphene quantum dot-modified electrode for monitoring of multivitamins in energy drinks. *Talanta* 252, 123836 <https://doi.org/10.1016/j.talanta.2022.123836>.
- Nafujjaman, M., Kim, J., Park, H.-K., Lee, Y.-K., 2018. Preparation of blue-color-emitting graphene quantum dots and their in vitro and in vivo toxicity evaluation. *J. Ind. Eng. Chem.* 57, 171–180. <https://doi.org/10.1016/j.jiec.2017.08.019>.
- Niu, F., Ying, Y.-L., Hua, X., Niu, Y., Xu, Y., Long, Y.-T., 2018. Electrochemically generated green-fluorescent N-doped carbon quantum dots for facile monitoring alkaline phosphatase activity based on the Fe³⁺-mediating ON-OFF-ON-OFF fluorescence principle. *Carbon* 127, 340–348. <https://doi.org/10.1016/j.carbon.2017.10.097>.
- Pan, D., Guo, L., Zhang, J., Xi, C., Xue, Q., Huang, H., Li, J., Zhang, Z., Yu, W., Chen, Z., Li, Z., Wu, M., 2012. Cutting sp₂ clusters in graphene sheets into colloidal graphene quantum dots with strong green fluorescence. *J. Mater. Chem.* 22, 3314. <https://doi.org/10.1039/c2jm16005f>.
- Papari, G.P., Gargiulo, V., Alfè, M., Di Capua, R., Pezzella, A., Andreone, A., 2017. THz spectroscopy on graphene-like materials for bio-compatible devices. *J. Appl. Phys.* 121, 145107 <https://doi.org/10.1063/1.4980106>.

- Qin, X., Zhan, Z., Zhang, R., Chu, K., Whitworth, Z., Ding, Z., 2023. Nitrogen- and sulfur-doped graphene quantum dots for chemiluminescence. *Nanoscale* 15, 3864–3871. <https://doi.org/10.1039/D2NR07213K>.
- Reghunath, B.S., Rajasekaran, S., Pinheiro, D., Jaleel, J.R., 2023. N-doped graphene quantum dots incorporated cobalt ferrite/graphitic carbon nitride ternary composite for electrochemical overall water splitting. *Int. J. Hydrogen Energy* 48, 2906–2919. <https://doi.org/10.1016/j.ijhydene.2022.10.169>.
- Ritter, K.A., Lyding, J.W., 2009. The influence of edge structure on the electronic properties of graphene quantum dots and nanoribbons. *Nat. Mater.* 8, 235–242. <https://doi.org/10.1038/nmat2378>.
- Shi, M., Zhu, H., Chen, C., Jiang, J., Zhao, L., Yan, C., 2023. Synergistically coupling of graphene quantum dots with Zn-intercalated MnO₂ cathode for high-performance aqueous Zn-ion batteries. *Int. J. Miner. Metall. Mater.* 30, 25–32. <https://doi.org/10.1007/s12613-022-2441-4>.
- Tetsuka, H., Asahi, R., Nagoya, A., Okamoto, K., Tajima, I., Ohta, R., Okamoto, A., 2012. Optically tunable amino-functionalized graphene quantum dots. *Adv. Mater.* 24, 5333–5338. <https://doi.org/10.1002/adma.201201930>.
- Vázquez-Nakagawa, M., Rodríguez-Pérez, L., Martín, N., Herranz, M.Á., 2022. Supramolecular assembly of edge functionalized top-down chiral graphene quantum dots. *Angew. Chem. -Int. Ed.* 61 <https://doi.org/10.1002/anie.202211365>.
- Wang, X., Bai, H., Shi, G., 2011. Size fractionation of graphene oxide sheets by pH-assisted selective sedimentation. *J. Am. Chem. Soc.* 133, 6338–6342. <https://doi.org/10.1021/ja200218y>.
- Wang, S., Chen, Z.-G., Cole, L., Li, Q., 2015. Structural evolution of graphene quantum dots during thermal decomposition of citric acid and the corresponding photoluminescence. *Carbon* 82, 304–313. <https://doi.org/10.1016/j.carbon.2014.10.075>.
- Wang, L., Wang, Y., Xu, T., Liao, H., Yao, C., Liu, Y., Li, Z., Chen, Z., Pan, D., Sun, L., Wu, M., 2014. Gram-scale synthesis of single-crystalline graphene quantum dots with superior optical properties. *Nat. Commun.* 5, 5357. <https://doi.org/10.1038/ncomms6357>.
- Wu, X., Ma, L., Sun, S., Jiang, K., Zhang, L., Wang, Y., Zeng, H., Lin, H., 2016. A versatile platform for the highly efficient preparation of graphene quantum dots: photoluminescence emission and hydrophilicity-hydrophobicity regulation and organelle imaging. *Nanoscale* 10, 1532–1539. <https://doi.org/10.1039/C7NR08093J>.
- Xu, Y., Wang, S., Hou, X., Sun, Z., Jiang, Y., Dong, Z., Tao, Q., Man, J., Cao, Y., 2018. Coal-derived nitrogen, phosphorus and sulfur co-doped graphene quantum dots: a promising ion fluorescent probe. *Appl. Surf. Sci.* 445, 519–526. <https://doi.org/10.1016/j.apsusc.2018.03.156>.
- Xu, L., Yang, X., Ding, H., Li, S., Li, M., Wang, D., Xia, J., 2019. Synthesis of green fluorescent carbon materials using byproducts of the sulfite-pulping procedure residue for live cell imaging and Ag⁺ ion determination. *Mater. Sci. Eng. c* 102, 917–922. <https://doi.org/10.1016/j.msec.2019.04.014>.
- Yan, Y., Chen, J., Li, N., Tian, J., Li, K., Jiang, J., Liu, J., Tian, Q., Chen, P., 2018. Systematic bandgap engineering of graphene quantum dots and applications for photocatalytic water splitting and CO₂ reduction. *ACS Nano* 12, 3523–3532. <https://doi.org/10.1021/acsnano.8b00498>.
- Yan, X., Cui, X., Li, L., 2010. Synthesis of large, stable colloidal graphene quantum dots with tunable size. *J. Am. Chem. Soc.* 132, 5944–5945. <https://doi.org/10.1021/ja1009376>.
- Yan, H., He, C., Li, X., Zhao, T., 2018. A solvent-free gaseous detonation approach for converting benzoic acid into graphene quantum dots within milliseconds. *Diamond Relat. Mater.* 87, 233–241. <https://doi.org/10.1016/j.diamond.2018.06.008>.
- Yan, H., Wang, Q., Wang, J., Shang, W., Xiong, Z., Zhao, L., Sun, X., Tian, J., Kang, F., Yun, S., 2023. Planted graphene quantum dots for targeted, enhanced tumor imaging and long-term visualization of local pharmacokinetics. *Adv. Mater.* 35, 2210809. <https://doi.org/10.1002/adma.202210809>.
- Ye, R., Xiang, C., Lin, J., Peng, Z., Huang, K., Yan, Z., Cook, N.P., Samuel, E.L.G., Hwang, C.-C., Ruan, G., Ceriotti, G., Raji, A.-R.-O., Martí, A.A., Tour, J.M., 2013. Coal as an abundant source of graphene quantum dots. *Nat. Commun.* 4, 2943. <https://doi.org/10.1038/ncomms3943>.
- Yew, Y.T., Loo, A.H., Sofer, Z., Klímová, K., Pumera, M., 2017. Coke-derived graphene quantum dots as fluorescence nanoquencher in DNA detection. *Appl. Mater. Today* 7, 138–143. <https://doi.org/10.1016/j.apmt.2017.01.002>.
- Yu, S., Zhong, Y.-Q., Yu, B.-Q., Cai, S.-Y., Wu, L.-Z., Zhou, Y., 2016. Graphene quantum dots to enhance the photocatalytic hydrogen evolution efficiency of anatase TiO₂ with exposed 001 facet. *Phys. Chem. Chem. Phys.* 18, 20338–20344. <https://doi.org/10.1039/C6CP02561G>.
- Zeng, G., Li, X.-X., Li, Y.-C., Chen, D.-B., Chen, Y.-C., Zhao, X.-F., Chen, N., Wang, T.-Y., Zhang, D.W., Lu, H.-L., 2022. A heterostructured graphene quantum dots/ β -Ga₂O₃ solar-blind photodetector with enhanced photoresponsivity. *ACS Appl. Mater. Interfaces* 14, 16846–16855. <https://doi.org/10.1021/acami.2c00671>.
- Zhang, R., Adsett, J.R., Nie, Y., Sun, X., Ding, Z., 2018. Electrochemiluminescence of nitrogen- and sulfur-doped graphene quantum dots. *Carbon* 129, 45–53. <https://doi.org/10.1016/j.carbon.2017.11.091>.
- Zhang, M., Bai, L., Shang, W., Xie, W., Ma, H., Fu, Y., Fang, D., Sun, H., Fan, L., Han, M., Liu, C., Yang, S., 2012. Facile synthesis of water-soluble, highly fluorescent graphene quantum dots as a robust biological label for stem cells. *J. Mater. Chem.* 22, 7461. <https://doi.org/10.1039/c2jm16835a>.
- Zhang, C., Cui, Y., Song, L., Liu, X., Hu, Z., 2016. Microwave assisted one-pot synthesis of graphene quantum dots as highly sensitive fluorescent probes for detection of iron ions and pH value. *Talanta* 150, 54–60. <https://doi.org/10.1016/j.talanta.2015.12.015>.
- Zhang, H., Guo, R., Li, S., Liu, C., Li, H., Zou, G., Hu, J., Hou, H., Ji, X., 2022. Graphene quantum dots enable dendrite-free zinc ion battery. *Nano Energy* 92, 106752. <https://doi.org/10.1016/j.nanoen.2021.106752>.
- Zhang, Y., Li, K., Ren, S., Dang, Y., Liu, G., Zhang, R., Zhang, K., Long, X., Jia, K., Zhang, Y., Li, K., Ren, S., Dang, Y., Liu, G., Zhang, R., Zhang, K., Long, X., Jia, K., 2019. Coal-derived graphene quantum dots produced by ultrasonic physical tailoring and their capacity for Cu(II) detection. *ACS Sustain. Chem. Eng.* 7, 9793–9799. <https://doi.org/10.1021/acssuschemeng.8b06792>.
- Zhao, M., 2018. Direct synthesis of graphene quantum dots with different fluorescence properties by oxidation of graphene oxide using nitric acid. *Appl. Sci.* 8, 1303. <https://doi.org/10.3390/app8081303>.
- Zhu, J., Tang, Y., Wang, G., Mao, J., Liu, Z., Sun, T., Wang, M., Chen, D., Yang, Y., Li, J., Deng, Y., Yang, S., 2017. Green, rapid, and universal preparation approach of graphene quantum dots under ultraviolet irradiation. *ACS Appl. Mater. Interfaces* 9, 14470–14477. <https://doi.org/10.1021/acami.6b11525>.
- Zhu, J., Wang, L., Gan, X., Tang, T., Qin, F., Luo, W., Li, Q., Guo, N., Zhang, S., Jia, D., Song, H., 2022. Graphene quantum dot inlaid carbon nanofibers: revealing the edge activity for ultrahigh rate pseudocapacitive energy storage. *Energy Storage Mater.* 47, 158–166. <https://doi.org/10.1016/j.ensm.2022.02.015>.